Materials Today Communications 37 (2023) 107242

Contents lists available at ScienceDirect

Materials Today Communications

journal homepage: www.elsevier.com/locate/mtcomm

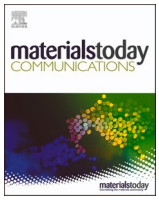

Hydrolytic degradation of polylactide/polybutylene succinate blends with bioactive glass

Inari Lyyra [a,*], Nina Sandberg [a], Vijay Singh Parihar [a], Markus Hannula [a], Heini Huhtala [a,b], Jari Hyttinen [a], Jonathan Massera [a], Minna Kellomäki [a]

[a] Faculty of Medicine and Health Technology, Tampere University, Tampere, Finland
[b] Faculty of Social Sciences, Tampere University, Tampere, Finland

ARTICLE INFO

Keywords:
Polylactide
Polybutylene succinate
Bioactive glass
Blends
Composites
Hydrolytic degradation
Mechanical properties
Tissue engineering

ABSTRACT

Polylactides (PLAs) have been vastly studied for biomedical engineering applications, but their rigidness limits their use. Blending them with more flexible polymers, such as polybutylene succinate (PBSu), results in softer materials, expanding the range of possible applications. However, the biopolymers lack bioactivity, which can be overcome by adding bioactive glass. Combining the inorganic phase with the organic phase (especially with blends) results in a complex material. Therefore, understanding the hydrolytic degradation of each component is crucial. In this context, we report on processing polylactide and polybutylene succinate (PLA/PBSu) blends and their composites (30 wt% of bioactive glass 13-93, BaG). The impact of blending and compounding with BaG on the final product's molecular weight and mechanical properties and the BaG dispersion in the polymer matrices was assessed. In addition, in vitro degradation in PBS was studied. While the degradation of the polymer was assessed by GPC, the BaG dissolution was quantified by ICP-OES. Blending decreased the initial mechanical properties and molecular weight, and compounding with BaG further decreased the initial mechanical properties. During the immersion in PBS, blending accelerated the loss of mechanical properties and molecular weight, while BaG accelerated the degradation of PLA-containing materials but had little effect on PBSu. Blending and compounding with BaG enabled us to produce materials with a wide range of mechanical properties: bending strength of 34–125 MPa, shear strength of 22–47 MPa and bending modulus of 1.1–3.9 GPa. The selection of tailorable properties of these polymer/BaG composites enables their application for tissue engineering of bone to soft tissue.

1. Introduction

Polylactides (PLAs) are biodegradable aliphatic polyesters vastly studied for bone, cartilage, tendon, vascular and neural tissue engineering [1]. However, they are tough and brittle, which limits their applications. One approach to improve the mechanical properties of PLAs is to blend them with soft polymers, e.g., polybutylene succinate (PBSu). PBSu has been mainly used as a commercial plastic but has recently gained interest in the biomedical field because of its high flexibility and good processability. PBSu-based scaffolds have shown promise for bone and soft tissue engineering applications [2–21].

PLA/PBSu blends have been mainly studied for packaging applications but have recently been evaluated for tissue engineering applications. Kanneci Altinişik et al. [22] evaluated PLLA/PBSu sponge scaffolds for neural tissue engineering. They reported that the scaffolds were not cytotoxic, and Schwann cells survived on them for 21 days. Abudula et al. [23] studied electrospun PLA/PBSu scaffolds for vascular tissue engineering. The blends showed superior cell attachment and proliferation compared to PLA or PBSu alone. Kimble and Bhattacharyya [24] reported the degradation behaviour of PLLA/PBSu blends for stent applications. Ojansivu et al. [25] reported enhanced cell attachment, proliferation and osteogenic differentiation of hASCs on knitted PLA/PBSu blends compared to plain PLA. Kun et al. [26] reported excellent biocompatibility of PLA/PBSu blends with L929 fibroblasts and bone marrow stem cells and in subcutaneous implantation in rats. Our recent article [21] demonstrated that culturing hASCs and hUCs on PLA/PBSu blend discs and PBSu discs promoted their viability and proliferation while maintaining their phenotype. In addition, the hASCs preserved their differentiation potential towards smooth muscle cells on the PBSu-containing discs, which is highly beneficial in soft tissue

* Corresponding author.
E-mail address: inari.lyyra@gmail.com (I. Lyyra).

https://doi.org/10.1016/j.mtcomm.2023.107242
Received 14 June 2023; Received in revised form 28 August 2023; Accepted 3 October 2023
Available online 5 October 2023

engineering.

Ideally, tissue-engineered constructs degrade at the same rate as the target tissues regenerate. Therefore, it is crucial to know the degradation rate of the materials used. However, only a few reports were found regarding the hydrolytic degradation of PLA/PBSu blends. Zhou et al. [27] reported that PLA/PBSu blends degraded faster than neat PLA and PBSu during 16 months in SBF. Wang et al. [28] studied the degradation of PLA/PBSu blends for 14 days in NaOH. The degradation was faster with increasing PBSu content in the blends. Kimble and Bhattacharyya [24] explored PLLA/PBSu blends as a stent material and reported that the blends exhibited a higher loss of mechanical properties and molecular weight than PLLA over 24 weeks in PBS.

In this study, a series of PLA/PBSu blends were manufactured, and their initial properties and hydrolytic degradation were studied. We hypothesised that when PBSu is added to PLA, the immiscibility of the two polymers would result in interphases between the blend components, accelerating the degradation of the blends.

In addition to blending PBSu with PLA, we also studied the effect of incorporating bioactive glass (BaG) into PLA, PBSu and the blends. It was hypothesised that by adjusting the blend composition and compounding with a ceramic filler, the selection of available degradation properties and mechanical properties would be further expanded, facilitating the selection of an ideal composition for different applications and target tissues. Composites of BaG and PLA or PBSu have exhibited decreased initial mechanical properties and accelerated degradation rates compared to neat PBSu and PLA [13], [29–33]. The accelerated degradation of the composites was mainly associated with increased hydrophilicity, higher degradation of the polymer during processing, increased porosity and the interactions between the glass dissolution by-products and the polymer matrix [17,29,31,32]. Furthermore, incorporating BaG into the blends would facilitate tailoring the material properties by releasing beneficial ions for the proliferation of the seeded cells in the scaffold. Regarding the degradation rate, we hypothesised that adding BaG would accelerate the degradation of the blends as the particles would induce more interfaces in the structure. To our knowledge, this is the first study to introduce PLA/PBSu blends with BaG.

2. Materials and methods

2.1. Materials

The biodegradable polymers used in the study were high purity, medical grade poly(L-lactide-co-D,L-lactide) 70/30 (PLA, Resomer LR 706 S, Evonik Industries AG, Darmstadt, Germany) and commercial grade polybutylene succinate (PBSu, Bionolle 1020 MD, Showa Denko Europe GmbH, Munich, Germany). The inherent viscosity of PLA was 4.0 dl/g (stated by the manufacturer) and 1.1 dl/g for PBSu, as measured by a viscometric analysis (Lauda PSV1, Lauda-Königshofen, Germany) with Ubbelohde capillaries (Schott-Instrument, Mainz, Germany) in chloroform at 25 °C. The BaG used in the composites was 13-93 (composition, in mol%, in Table 1). Analytical grade Na_2CO_3, $CaCO_3$, K_2CO_3, MgO, $CaHPO_4$-2 H_2O, and Belgian quartz sand were used to produce the glass. The glass was prepared and crushed in 125–250 μm particles as described in [29].

2.2. Manufacturing of polymer and composite rods

First, the PBSu granules were ground to approximately 1.5 mm grain size in a cutting mill (Fritsch Pulverisette, Fritsch GmbH, Idar-Oberstein, Germany). For manufacturing the blend composites, PLA and PBSu were weighed and manually premixed at appropriate weight ratios in glass bottles. Before processing, the ground polymers and glass particles were dried at 75 °C for 8 h in a vacuum oven. A custom-made laboratory scale co-rotating twin screw extruder (Mini ZE 20 *11.5 D, Neste Oy, Koelaitepalvelut, Porvoo, Finland) was used to melt-extrude cylindrical rods with a diameter of approximately 2 mm, under an N_2 protective gas. The materials were denoted as A/B(C), where A is the weight ratio of PLA (0, 50, 75 or 100 wt%), B is the weight ratio of PBSu (0, 25, 50 or 100 wt%), and C is added if the material contains BaG. The processing parameters for each composition are shown in Tables 2 and 3. After processing, the polymer rods were washed with ethanol in an ultrasonic cleaner and dried in a fume hood. All the rods were sealed in HDPE-bags and gamma irradiated for sterility with a minimum 25 kGy dose at BBF Sterilisationsservice GmbH (Kernen, Germany). All the extruded compositions were characterised as-processed for organic phase content, mechanical properties, and molecular weight and imaged using scanning electron microscopy (SEM) and X-ray micro-computed tomography (μ-CT).

Table 1
The nominal composition of the bioactive glass 13-93 in mol-%.

Glass	SiO_2	P_2O_5	CaO	Na_2O	MgO	K_2O
13-93	54.6	1.7	22.1	6.0	7.7	7.9

2.3. In vitro reactivity of the glass

The bioactivity of the composites, namely the formation of hydroxyapatite, was studied by immersing 30 mm long rods in 5 ml of simulated body fluid (SBF) for up to 14 days at 37 °C, in a shaking incubator (100RPM). The buffer volume (ml) to sample mass (g) ratio was more than 30:1, as suggested in the ISO 15814:1999. The SBF was prepared following the ISO/FDIS 23317 methodology, and all the containers used to prepare the buffer solution were rinsed with ethanol before use. The solution was not refreshed during the hydrolysis. At the end of each incubation period, the pH of the SBF was measured from three parallel samples using a Mettler Toledo pH meter, and the ion release was measured using inductively coupled plasma - optical emission spectrometry (ICP-OES). Ions released from the BaG into the buffer solution were quantified with ICP-OES 5110 (Agilent Technologies Inc., Santa Clara, CA, USA). 2 ml of the buffer solution was collected at each time point and diluted with 8 ml of 1 M nitric acid (Romil Ltd., Cambridge, UK) for the measurement of following wavelengths: Ca 393.366 nm, K 766.491 nm, Mg 279.553 nm, P 253.561 nm, and Si 250.690 nm. The means of three parallel samples were calculated and presented with their standard deviation.

2.4. Hydrolytic degradation

The hydrolytic degradation of the materials was studied by placing 70 mm long samples in 12 ml of phosphate-buffered saline (PBS) at 37 °C in a shaking incubator for up to 24 weeks. The buffer volume to sample mass ratio in the PBS study was also according to the suggestion of ISO 15814:1999. The number of parallel samples was six. The PBS was prepared by dissolving 5.9 g sodium chloride, 0.755 g mono- and 3.54 g disodium phosphate into 1 l of deionised water and adjusting the pH to 7.4. All the containers used to prepare the buffer solution and the test tubes were rinsed with ethanol to prevent contamination. The buffer solution was changed every two weeks. At the same time, the pH was

Table 2
The rods' nominal weight ratios of PLA, PBSu, and 13-93.

Material	PLA (wt%)	PBSu (wt%)	13-93 (wt%)
100/0	100	0	0
75/25	75	25	0
50/50	50	50	0
0/100	0	100	0
100/0C	100	0	30
75/25C	75	25	30
50/50C	50	50	30
0/100C	0	100	30

Table 3
The processing parameters of the polymer and composite rods of the study.

	100/0	75/25	50/50	0/100	100/0C	75/25C	50/50C	0/100C
Temperature (°C)	195–222	193–220	195–229	95–115	187–220	155–180	155–176	100–115
Pressure (psi)	430–530	300–360	60–80	190–210	230–330	500–590	280–380	225

measured, and 2 ml of buffer solution was collected for the ion release measurements from three parallel samples. At the end of each time point, pH, water absorption, mass loss, molecular weight, mechanical properties, ion release in the buffer solution, and dimension changes were studied. After the last time point, the samples were also imaged with SEM and μ-CT.

2.5. Water absorption and mass loss

The starting weights of the samples were measured before the immersion, and the samples were weighed after mechanical testing and blot drying to measure the wet mass at each time point. Then, the samples were rinsed twice with deionised water and once with ethanol before drying them overnight in a laminar hood, followed by drying for a week in a vacuum chamber and weighing again (dry mass). The 24-week samples were dried in a vacuum chamber for two weeks to ensure they were dry before weighing. There were six parallel samples for the water absorption (WA) and mass loss. The WA and mass loss were calculated using the following formulae:

$$Water\ absorption\ (WA) = \frac{wetmass_{final} - drymass_{final}}{drymass_{final}} \times 100\% \quad (1)$$

$$Mass\ loss = \frac{drymass_{initial} - drymass_{final}}{drymass_{initial}} \times 100\% \quad (2)$$

2.6. Mechanical properties

The initial mechanical properties (bending strength, bending modulus, and shear strength) were measured for the non-immersed samples as non-sterile, sterile, dry, and wet. The wet samples were immersed in PBS for one hour and blot-dried before testing. In addition, at each time point of the hydrolysis, the samples were mechanically tested to monitor their mechanical strength retention as a function of the immersion time. The mechanical properties (bending and shear strength and bending modulus) during the immersion in PBS are presented in relative terms normalised to the initial values. The retention time is defined as when there were no significant differences in the mechanical properties compared to the initial values, i.e. the material retained its initial mechanical properties.

The in vitro samples were tested wet after blot drying. The testing was conducted at room temperature using an Instron 4411 (Instron Ltd., High Wycombe, UK) material testing machine. The sample diameters were measured before the testing. The bending properties were measured with a 3-point bending test, as in [30]. The bending span was 32 mm, and the crosshead speed was 5 mm/min. In the shear test, the crosshead speed was 10 mm/min, and the testing was conducted as in [30]. The bending strength, bending modulus, and shear strength were calculated using the formulae below:

Bending strength, σ_f [MPa]:

$$\sigma_f = \frac{8 \bullet F_{max} \bullet L}{\pi \bullet d^3} \quad (3)$$

Bending modulus, E [GPa]:

$$E = \frac{4 \bullet slope \bullet L^3}{3 \bullet \pi \bullet d^4} \bullet \frac{1}{1000} \quad (4)$$

Shear strength, τ [MPa]:

$$\tau = \frac{2 \bullet F_{max}}{\pi \bullet d^2} \quad (5)$$

where F_{max} = applied maximum force in testing [N], L = support span [mm], d = diameter of the rod [mm]. The results are given as means of six measurements with the standard deviation.

2.7. Inorganic phase content

The amount of inorganic phase in the composites was measured before the hydrolysis in PBS by thermal gravimetric analysis (TGA Q500, TA Instruments, New Castle, DE, USA). In this case, the temperature was raised to 700 °C at 20 °C/min in air.

2.8. Thermal properties

The thermal properties of the neat polymers, blends and composites were measured before and after immersion by differential scanning calorimeter (DSC) TAinstruments Q1000 (TAinstruments, New Castle, DE, USA). The samples after immersion were dried and handled similarly to the mass loss samples before measuring dry mass. The number of parallel samples was two. Approximately 5 mg of the samples were weighed in a standard aluminium crucible and measured with one of the following methods: 1) cooled to − 20 °C, heated to 200 °C at a rate of 20 °C/min, stabilized for 1 min, cooled to − 20 °C a rate of 50 °C/min, stabilized for 1 min, and heated again to 200 °C at 20 °C/min, or 2) cooled to − 75 °C, stabilised for 1 min, heated to 200 °C at a rate of 20 °C/min, cooled to − 75 °C a rate of 50 °C/min, stabilised for 1 min, and heated again to 200 °C at 20 °C/min. Method 2 was used only for determining the T_m of 0/100 samples after 24 weeks because of high variability and disturbances in the thermograms with the measurements starting from − 20 °C. All thermal cycles were performed in a nitrogen atmosphere. The melting temperature, $T_{m,}$ was obtained from the first heating cycle and the glass transition temperature, T_g, from the second heating cycle. The data was analyzed using Universal Analysis software.

The melting enthalpy (ΔH) was calculated using the following equation:

$$\Delta H = \Delta H_m - \Delta H_c \quad (6)$$

where ΔH_m is the melting enthalpy, and ΔH_c is the enthalpy of cold crystallisation.

2.9. Dimensional stability

The diameters of six parallel samples were measured as dry before the hydrolysis and wet before mechanical testing after each time point. The diameters were measured using a digital calliper from three points in each sample.

2.10. Nuclear magnetic resonance analysis

Proton nuclear magnetic resonance (NMR) analysis was used to determine each polymer's ratios in the blends and blend composites. 10 mg blend samples were fully dissolved in 800 μl of $CDCl_3$ and transferred to an NMR tube. All proton NMR were recorded using the JEOL-500 MHz instrument (SCZ500R, JEOL Resonance, Japan) in $CDCl_3$.

The ratio of each polymer component in the blend was calculated

from peak integration from PLA and PBSu. Fig. 1 shows an example of an NMR spectrum obtained from a 50/50 blend before immersion with all the peaks from both polymers. The peaks chosen for the analysis were the peak at 1.84 (noted as B in Fig. 1), representing the PLA component due to 6 protons of the methyl group in the polymer repeating unit, and the peak at 1.7 (noted as b in Fig. 1), representing PBSu due to 4 protons from the ethylene group in the polymer repeating unit. The integration of these two peaks was selected for the polymer ratio calculation in all samples.

2.11. Molecular weight

The degradation of the PLA and PBSu in the samples was monitored with gel permeation chromatography (GPC, Shimadzu Prominence, Tokyo, Japan) at each time point of the hydrolysis in PBS. Approximately 7.5 mg of the polymer and 10.7 mg of the composite samples were dissolved into 5 ml of HPLC-grade chloroform. The filtered (0.2 μm) samples were run through two Shodex GPC KF-806 M columns and a Shodex GPC KF-G 4.6 × 10 mm pre-column. The composite samples were filtered twice. The eluent was chloroform flowing at a rate of 1 ml/min. Narrow PDI polystyrene standards with a range of 1 370–2 480,000 Da were used for calibration. The M_n and M_w are presented as means of two parallel samples with standard deviation. The parallel samples were independently prepared, and one injection per sample was used.

Because the chromatograms of the blends exhibited only a single peak, the molecular weight of each component (PLA and PBSu) was estimated as follows. First, NMR was used to measure the blending ratio of the blends. Both the initial blending ratios and the ratios after in vitro were measured. The molecular weights of the blends obtained by GPC were analysed separately using the Mark-Houwink constants of PS, PLA, and PBSu (Table 4) and then multiplied by the respective fraction obtained from NMR analysis. A similar approach was used in [34].

2.12. Electron microscopy and elemental analysis

The samples cross section was imaged, before and after immersion in PBS, by scanning electron microscopy using a Zeiss Crossbeam 540 (Carl Zeiss AG, Jena, Germany) and elemental analysis performed with a X-Max-80 EDX detector (Oxford Instrument plc, Abingdon, UK). The accuracy of the elemental analysis was 1–2 wt%. The samples were embedded in epoxy and polished before imaging.

Table 4
The Mark-Houwink constants used in molecular weight calculations.

Polymer	α	K
Polystyrene	0.73[a]	0.000112[a]
Polylactide	0.73[b]	0.000545[b]
Polybutylene succinate	0.71[c]	0.0000631[c]

[a] [35],
[b] [36],
[c] [37].

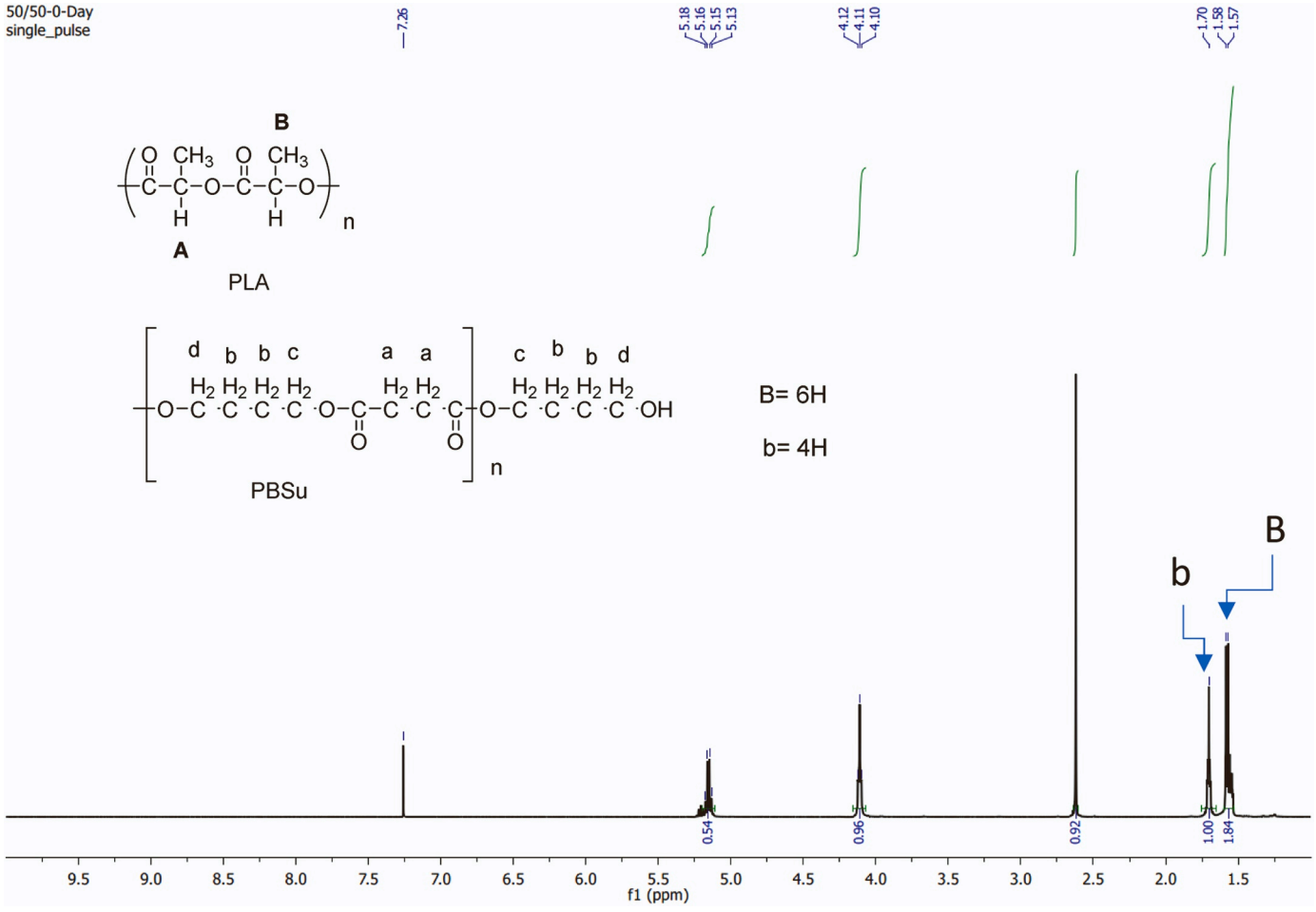

Fig. 1. An example of a 50/50 blend ^{1}H NMR spectrum before immersion. The peaks for calculating the polymer ratios in the blends are denoted as b (PBSu peak, 4 protons) and B (PLA peak, 6 protons).

2.13. X-ray micro-computed tomography

The BaG particle distribution in the composites was assessed by X-ray micro-computed tomography (μ-CT) using MicroXCT-400 (Carl Zeiss X-ray Microscopy Inc., Pleasanton, CA, USA). The tube voltage was 60 kV, the current 167 μA and the pixel size was 2.27 μm. The datasets were cropped to 1×1×2 mm cuboids for analysis and visualised with Avizo 2020.2 Software (Thermo Fisher Scientific, Waltham, MA, USA).

2.14. Statistical analysis

The mechanical testing (bending strength, bending modulus, and shear strength) data, mass loss, and water absorption results were statistically analysed with SPSS Statistics 25 (IBM, Armonk, NY, USA). All quantitative data are presented as means with standard deviation. All the measurements mentioned above were conducted with six parallel samples with each material (n = 6). The data were statistically analysed with a non-parametric Kruskal-Wallis test. The Bonferroni correction based on the number of planned comparisons minimises the error produced by familywise calculations. The comparisons were made within two groups: polymers with each other and composites with each other. In addition, pairwise comparisons with corresponding polymers and composites were made. The results were considered statistically significant when the adjusted p-value was < 0.05.

3. Results

3.1. Characterisation of the polymer and composite rods after processing

PLA, PBSu, two PLA/PBSu blends (75/25 and 50/50), and their composites were processed. The composites were characterised for their initial inorganic phase content (Table 5). The nominal inorganic phase content of all composites was 30 wt%. In 100/0C, 50/50C, and 0/100C, the variation between the nominal and measured values was ± 5 wt%, while 75/25C had a maximum of 12 wt% higher inorganic phase content than the nominal value.

The initial blending ratios were measured with NMR and used in the molecular weight calculations. The initial blending ratios of 75/25 and 50/50 were 82/18 and 55/45, respectively, and the initial blending ratios of 75/25C and 50/50C were 69/31 and 61/39, respectively (Table 6). The molecular weights of the materials were measured to assess the polymer degradation induced by melt processing and gamma irradiation (Fig. 2). Gamma irradiation decreased the initial molecular weight of both as-processed PLA and PBSu, but PBSu was less affected than PLA. During processing, the molecular weight of PLA decreased by 56% (M_n) and 53% (M_w), and the molecular weight of PBSu decreased by 38% (M_n) and 36% (M_w).

Blending accelerated the molecular weight decrease of both PLA and PBSu during the manufacturing of the rods. In 75/25, the PLA molecular weight decreased by 88% (M_n) and 70% (M_w), and in 50/50 by 93% (M_n) and 85% (M_w) after processing, compared to raw material. PBSu's initial molecular weight decreased more with a higher PLA content in the blend. In 75/25, it decreased by 80% (M_n) and 45% (M_w), and in 50/50, by 60% (M_n) and 3% (M_w).

Introducing BaG to PLA increased PLA's thermal degradation during the 100/0C sample manufacturing. The molecular weight of PLA decreased by 66% (M_n) and 67% (M_w) in 100/0C during processing. The PBSu molecular weight in PBSu/BaG composites did not notably change in processing by adding BaG.

Compounding BaG with the blends decreased the PLA molecular weight during processing more when compared to 100/0C, but the decrease was similar in 75/25C and 50/50C. In 75/25C, PLA initial molecular weight decreased by 92% (M_n) and 82% (M_w) and in 50/50C, 93% (M_n) and 83% (M_w). Compounding with BaG did not affect the molecular weight decrease of PBSu when processing the blend composites.

The initial mechanical properties of the neat polymers and blends decreased with increasing PBSu content (Fig. 3). The initial bending strength and modulus of 100/0 were 125 MPa and 3.9 GPa, respectively. With 25% addition of PBSu, they decreased by 22% and 28%, and with 50% addition, by 36% and 46%, respectively. The initial bending strength and modulus of 0/100 were 47 MPa and 1.0 GPa, respectively. The bending strength and bending modulus of 100/0 were statistically higher than 0/100 (both $p < 0.001$), and the modulus was higher than 50/50 ($p < 0.05$). In addition, the bending strength and modulus of 75/25 were higher than 0/100 ($p < 0.001$ and $p < 0.05$, respectively). No statistical differences were noted between the polymers' initial shear strength.

Compounding with BaG decreased the bending strength by 27–45% and shear strength by 18–45% (Fig. 3a-b). The bending and shear strength of 75/25 was higher compared to 75/25C ($p < 0.05$ and $p < 0.001$, respectively), and 100/0 had a higher shear strength compared to 100/0C ($p < 0.05$). The effect of BaG on the bending and shear strength was similar in the blend composites and neat polymer composites. The bending modulus was less affected by the addition of BaG than the bending and shear strength, and the moduli of the composites and corresponding polymers did not statistically differ (Fig. 3c). The bending strength and modulus of 100/0C were statistically higher compared to 0/100C (both $p < 0.05$).

The thermal properties of the polymers and composites were measured to get more insight into the materials' miscibility and degradation behaviour. The PLA was completely amorphous, with only a T_g in the thermograms. For PBSu, the situation was the opposite, and despite additional DSC runs starting from − 75 °C, the glass transition of PBSu could not be reliably analysed, as previously reported in [38]. 75/25 and 50/50, and the corresponding composites showed the T_g close to that of the PLA. The T_g of neat PLA is 59.4 °C, which decreased to 55.1 °C and 54.2 °C with 25% and 50% addition of PBSu, respectively (Table 7). BaG did not influence the PLA T_g, and the decrease in T_g was similar in the blend composites and the neat blends.

The influence of blending on the melting peak and melting enthalpy of the materials was also assessed. Neat PLA was amorphous, and thus, its T_m could not be evaluated. Neat PBSu showed a T_m at 119 °C (Table 8). The blends showed a slightly lower T_m than neat PBSu, 114.7 °C and 114.1 °C for 75/25 and 50/50, respectively. BaG did not have a significant effect on the T_m of the materials. The ΔH of neat PBSu was 70.8 J/g, and the blends showed much lower values, 16.2 J/g for 75/25 and 37.9 J/g for 50/50. BaG decreased the melting enthalpy of PBSu to 47.0 J/g. Compounding the blends with BaG induced a small cold crystallisation peak, considered in the enthalpy calculations (Eq. 6). The blend composites also showed lower melting enthalpies than the

Table 5
Initial inorganic phase content in the composites. n = 6.

Material	100/0C	75/25C	50/50C	0/100C
Nominal inorganic phase content (wt%)	30	30	30	30
Measured inorganic phase content (wt%)	28.1–34.4	24.9–42.4 *	27.9–36.5	27.9–32.3 * *

* n = 10, * * n = 8

Table 6
PLA/PBSu ratios of the blends and the blend composites measured by nuclear magnetic resonance before immersion and at each time point. n = 2.

Time point (weeks)	75/25	50/50	75/25C	50/50C
0	82/18	55/45	69/31	61/39
3	81/19	57/43	72/28	57/43
6	80/20	56/44	66/34	56/44
12	80/20	56/44	69/31	57/43
24	82/18	57/43	66/34	55/45

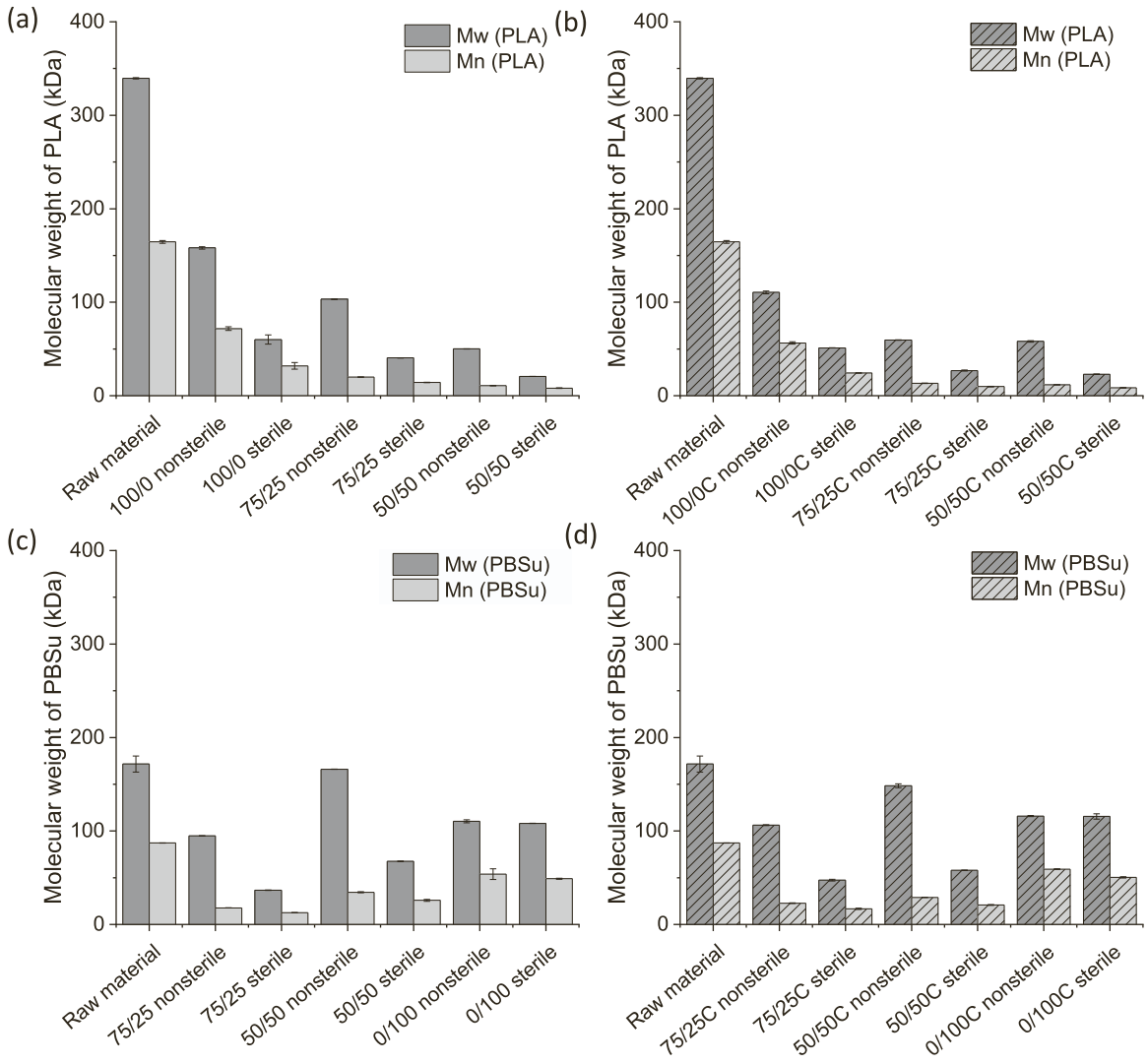

Fig. 2. Weight-average (M_w) and number-average (M_n) molecular weight of as-processed (a) neat PLA and PLA in blends, (b) PLA in composites, (c) neat PBSu and PBSu in blends, and (d) PBSu in composites. n = 2. The results are presented as means with standard deviation.

corresponding polymers, 13.4 J/g and 18.8 J/g, respectively.

3.2. In vitro reactivity of the glass

The pH of the SBF stayed within the 7.4 ± 0.2 range even after 14 days, and there were no differences between the materials (data not shown). The release rate of Ca, Mg, and K ions was quicker for the first 3 days and then slowed down (Fig. 4). In addition, their release profiles were independent of the matrix. The release of P plateaued after three days with 75/25C and 50/50C. The release of Si was higher with the blend composites compared to the neat polymer composites, and 75/25C had the highest release of Si.

3.3. Hydrolysis in phosphate-buffered saline

The materials were immersed in PBS for up to 24 weeks to study the effects of blending and compounding with BaG on the hydrolytic degradation rates of the materials. The neat polymers and blends did not induce notable pH changes during the 24 weeks (data not shown). Incorporating BaG increased the pH of the PBS from 7.40 to 7.75 at two weeks (Fig. 5). The effect was slightly higher with 75/25C and 50/50C (the increases of 0.35 and 0.25, respectively) compared to 100/0C and 0/100C.

3.4. Water absorption

The neat polymers and blends absorbed only a little water (1–7%) over 24 weeks in PBS (Fig. 6). Compounding with BaG increased the WA of the materials to 9–113 wt% in 24 weeks. 100/0C absorbed the most water, up to 113 wt% at 24 weeks ($p < 0.001$ compared to 100/0). 75/25C and 50/50C absorbed significantly more water at 3 and 6 weeks in vitro than 75/25 and 50/50 ($p < 0.001$ and $p < 0.01$ at three weeks, both $p < 0.001$ at 6 weeks, respectively). At 12 weeks, 100/0C and 75/25C had higher WA than 100/0 and 75/25, respectively (both $p < 0.001$).

3.5. Mass loss

The mass loss of the neat polymers and blends was negligible, but compounding with BaG increased the mass loss of the materials to 3–11 wt% at 24 weeks (Fig. 7). The effect was most apparent in the blend composites; 75/25C and 50/50C lost more mass after three weeks than the other materials (both $p < 0.05$ at 6 weeks compared to 100/0C). 75/25C lost more mass than 75/25 at all time points after 3 weeks ($p < 0.001$). 50/50C lost more mass than 50/50 at 6 weeks ($p < 0.05$), and 100/0C lost more mass than 100/0 at 24 weeks ($p < 0.05$).

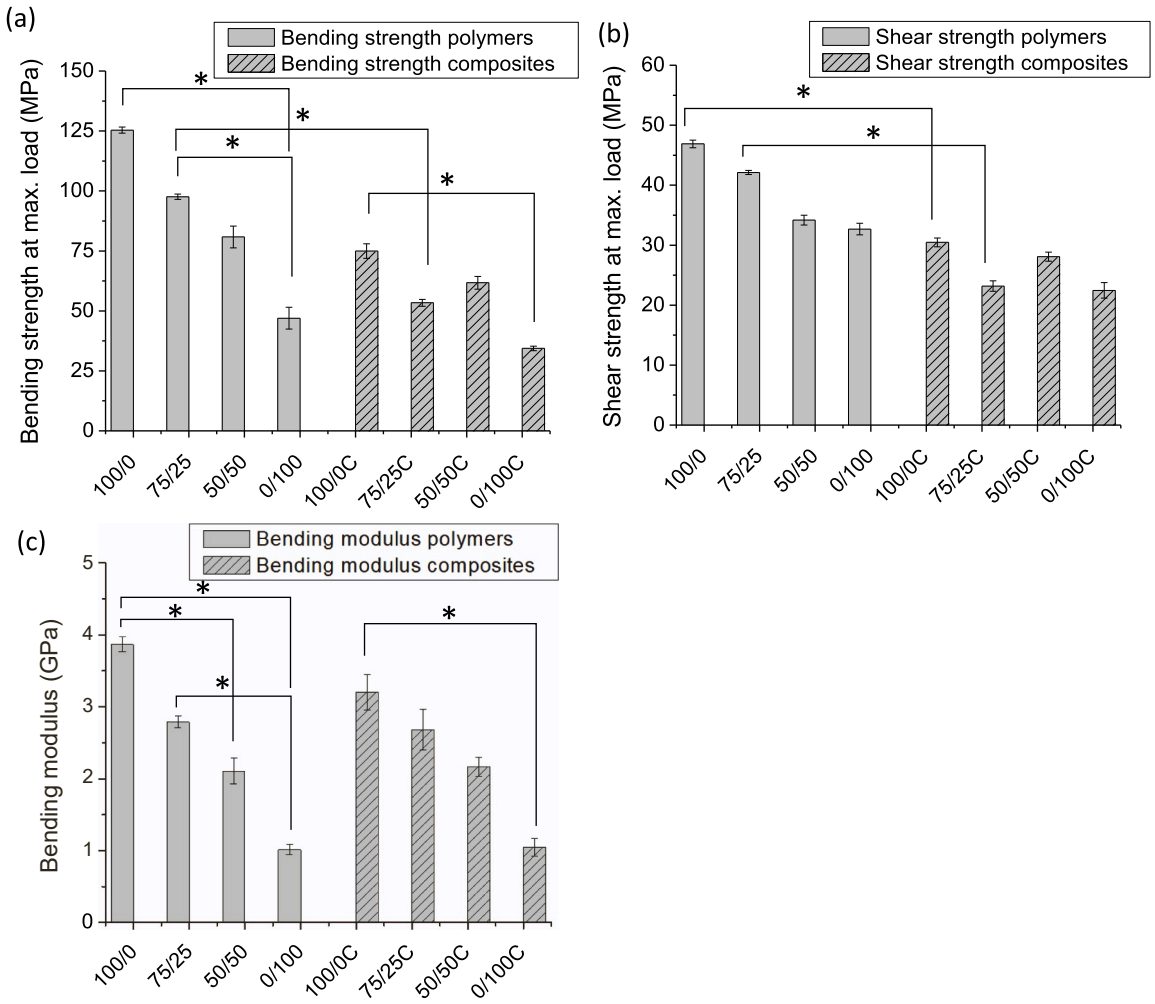

Fig. 3. Initial bending strength (a), shear strength (b) and bending modulus (c) of the as-processed rods. The results are presented as means with standard deviation. * $p < 0.05$. $n = 6$.

Table 7
The glass transition temperatures of the polymers and composites before and after 24 weeks in vitro. $n = 2$. The results are presented as means with standard deviation.

	PLA T_g midpoint before immersion (°C)		PLA T_g midpoint after immersion (°C)	
Sample	Mean	SD	Mean	SD
100/0	59.4	0.1	55.1	0.6
75/25	55.1	0.1	29.7	0.7
50/50	54.2	0.2	40.2	0.3
100/0C	59.7	0.4	54.0	0.4
75/25C	55.3	0.7	47.0	1.1
50/50C	56.4	0.3	48.6	0.4

3.6. Dimensional changes

Dimensional changes of the rods were studied by measuring their diameter wet before mechanical testing at each time point. The polymers exhibited minor dimensional changes during immersion (Fig. 8). The composites showed more dimensional changes compared to the polymers. At three weeks, 100/0C had shrunk 8% compared to its initial diameter ($p < 0.05$ compared to 100/0). At 6 weeks, 75/25C had swollen 6%, which was statistically significant compared to the other composites ($p < 0.05$, except for 0/100C $p < 0.001$). At 12 weeks, 100/0C and 75/25C had swollen 10% and 9%, respectively ($p < 0.001$ compared to 100/0 and 75/25). At 24 weeks, 100/0C had swollen the most, 44% in diameter ($p < 0.001$ compared to 100/0). It was also noted that 100/0C rods did not only swell the most in diameter but also increased in length during the hydrolysis. The samples reached a length of 75 mm and 90 mm at 12 and 24 weeks, respectively, corresponding to 7% and 30% increases in length. The other composites had swollen 12–22% in diameter at 24 weeks without a notable increase in length.

3.7. Mechanical properties

Neat PLA and PBSu retained at least 70% of their initial bending strength for at least 12 weeks in vitro (Fig. 9a). At 3 weeks, 100/0 had significantly more initial bending strength left than 0/100 ($p < 0.05$). Blending with 25% of PBSu did not affect the bending strength retention of PLA, but the 50% addition of PBSu shortened the bending strength retention time to at least 6 weeks. After 3 weeks, no significant differences between materials and within time points were seen, and at 24 weeks, all the neat polymers and blends had 31–38% of their initial bending strength left.

BaG accelerated the loss of mechanical properties during immersion in PBS (Fig. 9b), shortening the bending strength retention of all the PLA-containing composites to six weeks. Compounding with BaG had no effect on the bending strength retention of neat PBSu. At three weeks, 0/100C retained its bending strength significantly better than 75/25C and 50/50C ($p < 0.05$ and $p < 0.001$, respectively). No significant differences between the materials were seen after 3 weeks in vitro, and at 24 weeks, the composites had 4–12% left of their initial bending strength.

Table 8
The PBSu crystallinity before and after 24 weeks in vitro. n = 2. The results are presented as means with standard deviation.

	Before immersion				After immersion			
	T_m (°C)		ΔH_m (J/g)		T_m (°C)		ΔH_m (J/g)	
Sample	Mean	SD	Mean	SD	Mean	SD	Mean	SD
100/0	amorph.	-	amorph.	-	amorph.	-	amorph.	-
75/25	114.7	0.6	16.2	0.7	109.1	0.3	21.7*	1.5
50/50	114.1	1.2	37.9	0.1	113.8	0.5	35.0*	0.5
0/100	119.0	2.2	70.8	0.8	115.9 * *	2.4	83.9 * *	2.0
100/0C	amorph.	-	amorph.	-	amorph.	-	amorph.	-
75/25C	114.6	0.5	13.4*	0.8	113.8	0.1	16.4*	0.4
50/50C	116.0	1.4	18.8*	1.3	114.5	0.4	23.1*	0.5
0/100C	118.0	2.1	47.0	1.1	117.9	0.3	52.9	1.6

* Cold crystallisation taken into account * * Acquired from runs started from − 75 °C

The bending strength of the corresponding polymers and composites were also compared pairwise (Fig. 9c-f). BaG shortened the bending strength retention of all PLA-containing materials. 100/0 retained its bending strength better than 100/0C from 12 weeks (12 and 24 weeks $p < 0.001$) and 75/25 from 6 weeks ($p < 0.001$, except $p < 0.05$ at 24 weeks). BaG did not affect the bending strength retention of 0/100 and had only a minor effect on the bending strength of 50/50. Between 50/50 and 50/50C, there was a statistical difference only at 6 weeks ($p < 0.001$).

Similarly to the bending strength, a 25% addition of PBSu did not affect the shear strength retention of the PLA (Supplementary file, Fig. S1a). 100/0 and 75/25 retained their shear strength for 12 weeks in vitro (at three weeks, 75/25 had more of its initial shear strength left than 50/50, $p < 0.05$). Similarly, the materials with a higher PBSu content, 50/50 and 0/100, retained their initial shear strength for 6 and 12 weeks in vitro, respectively. At 12 weeks, 50/50 had 66% left of its initial shear strength, and 0/100 had 38% left, less than all other materials ($p < 0.001$ compared to 100/0 and 75/25, $p < 0.01$ to 50/50). At 24 weeks, the neat polymers and blends had 21–39% left of their initial shear strength. 100/0 had significantly more of its initial shear strength left than 75/25 ($p < 0.001$) and 0/100 ($p < 0.05$), and 50/50 more than 75/25 ($p < 0.05$).

BaG had a similar effect on the shear strength of the PLA-containing materials as it had on the bending strength; it shortened their shear strength retention to six weeks (Supplementary file, Fig. S1b). As opposed to bending strength, BaG shortened the shear strength retention of 0/100C to six weeks. 50/50C lost 25% of its initial shear strength at three weeks ($p < 0.01$ compared to 100/0C and 0/100C). At 6 and 12 weeks, there were no significant differences between the materials. After 24 weeks in vitro, the composites had 6–31% of their initial shear strength left. 100/0C had the least of its initial shear strength left ($p < 0.05$ for 75/25C and $p < 0.001$ for 50/50C). In pairwise comparisons between the corresponding polymers and composites (Supplementary file, Fig. S1c-f), 100/0C lost its shear strength quicker compared to 100/0 ($p < 0.05$ at 6, 12, and 24 weeks). 75/25 and 50/50 had statistically higher strength retention than their composites only at 6 weeks (both $p < 0.05$). There were no significant differences in the shear strength retention between 0/100 and 0/100C at any time.

All the polymers retained at least 80% of their initial bending modulus for the duration of the study (Fig. 10a). No significant differences were seen between the polymers within any time point. Compounding with BaG decreased the bending modulus retention time of 100/0C to at least 6 weeks and that of 50/50C to at least 3 weeks (Fig. 10b). In the case of 75/25C and 0/100C, BaG did not affect the bending modulus retention. Looking at the differences between materials within the time points, at 6 weeks and 24 weeks, 0/100C retained its bending modulus significantly better than the other materials ($p < 0.001$ for 100/0C, $p < 0.01$ for 75/25C, $p < 0.01$ for 50/50C at 6 weeks, and $p < 0.05$ at 24 weeks). At 12 weeks, 0/100C retained its bending modulus significantly better than 100/0C ($p < 0.05$).

In the pairwise comparisons between each polymer and corresponding composite (Fig. 10c-f), 100/0 retained its bending modulus significantly better than 100/0C, with statistically different values from 12 weeks onwards ($p < 0.01$ at 12 weeks and $p < 0.05$ at 24 weeks), and 75/25 retained its bending modulus significantly better than 75/25C, with statistically different values from 6 weeks onwards ($p < 0.05$ at 6 and 24 weeks, $p < 0.001$ at 12 weeks). The addition of glass did not influence the bending modulus retention of 50/50 or 0/100.

3.8. Molecular weight

The degradation of each polymer component in the blends and composites was assessed by measuring the molecular weight of the materials at each time point. The blending ratios of the blends and blend composites measured by NMR and used in the molecular weight calculations are presented in Table 6. No clear trends in the blending ratios were seen as a function of the immersion time. The molecular weights of PLA and PBSu decreased steadily in neat polymers and blends. PLA had 18–29% (M_n) and 12–27% (M_w), and PBSu had 17–39% (M_n) and 11–34% (M_w) of their initial molecular weight left after 24 weeks in vitro (Fig. 11). Blending accelerated the degradation of both PLA and PBSu. After three weeks of immersion, the molecular weights of both PLA and PBSu were lower in the blends than in neat PLA and PBSu. The PLA M_n decreased the quickest in 75/25, reaching 18% at 24 weeks. The PLA M_w decreased the fastest in 50/50, which had 12% left of its initial M_w at 24 weeks. PBSu exhibited a similar trend, the PBSu M_n of 75/25 reaching 17% at 24 weeks and 50/50 retaining 11% of its initial PBSu M_w at 24 weeks.

Compounding with BaG slowed the molecular weight decrease of both PLA and PBSu in the blend composites (Fig. 11). However, in 100/0C and 0/100C, BaG accelerated the polymer degradation. In the composites, PLA retained 18–37% of its initial M_n and 18–33% of its initial M_w after 24 weeks in vitro. At the same time, PBSu retained its molecular weight in the composites slightly better, having 36–49% of its initial M_n and 34–43% of its initial M_w left. PLA and PBSu retained their molecular weight in 50/50C better than in the other composites.

3.9. Thermal properties

The immersion in PBS for 24 weeks decreased the PLA T_g by 4.3–5.7 °C in 100/0 and 100/0C (Table 7). The decreases in the blends were much higher, 25.4 °C in 75/25 and 14.0 °C in 50/50. The PLA T_g in 75/25C and 50/50C decreased by 8.3 and 7.8 °C during immersion, respectively. The neat PLA and 100/0C were still amorphous after the immersion.

All the PBSu-containing materials showed a T_m in their thermograms also after immersion. In addition, all the blends and blend composites exhibited a cold crystallisation peak. Furthermore, a shoulder on the right side of the melting peak was detected for 75/25. The immersion in PBS decreased the T_m of 0/100 by 3 °C and the T_m of 75/25 by 6 °C. It

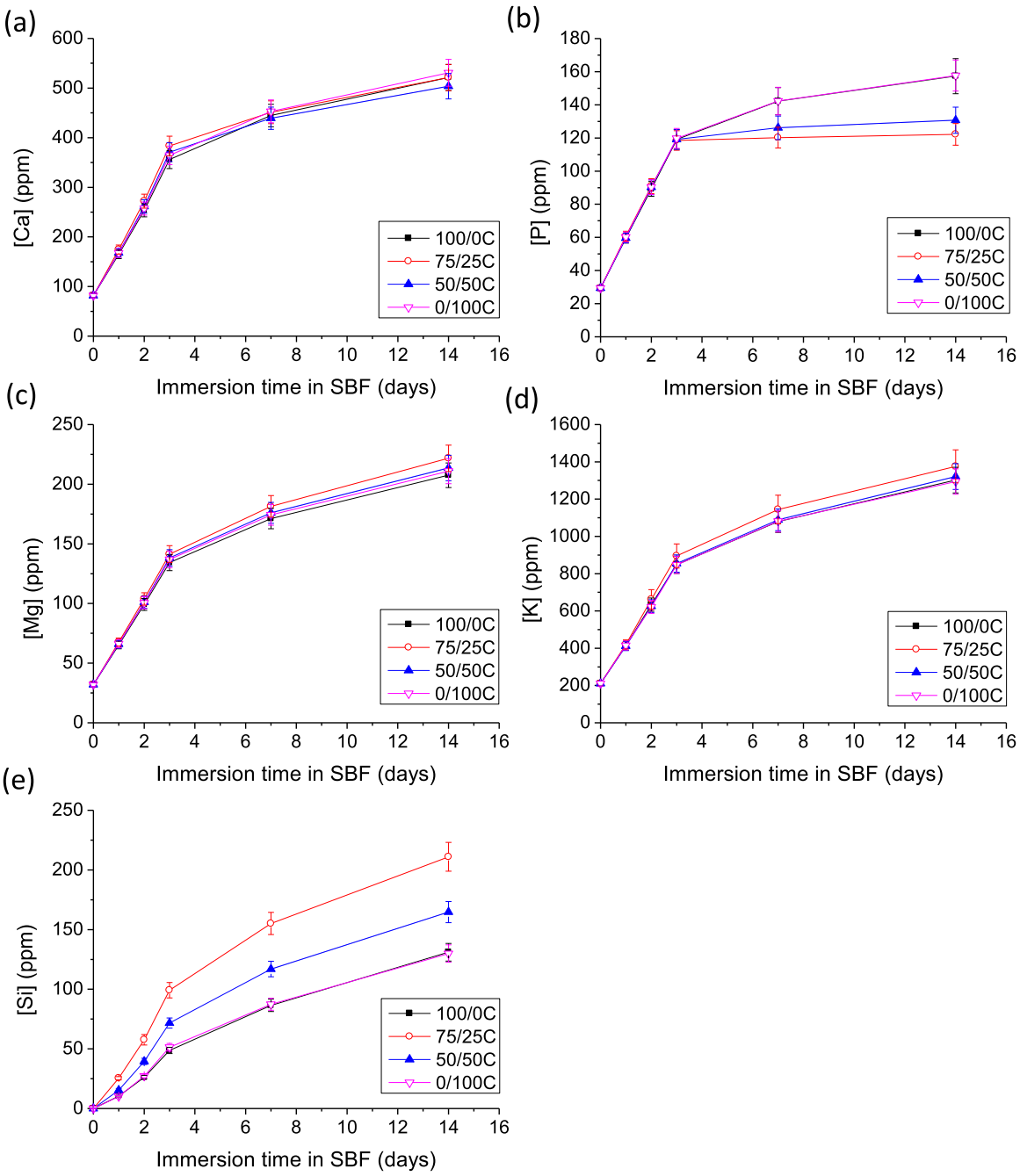

Fig. 4. (a) Calcium (Ca), (b) phosphorus (P), (c) magnesium (Mg), (d) potassium (K) and (e) silicon (Si) ion release from the composites into the SBF over 14 days. n = 3. The results are presented as means with standard deviation. Note the different scales in y-axes.

did not affect the T_m of the other materials. The melting enthalpy of neat PBSu increased by 13 J/g after 24 weeks in PBS, but the immersion did not significantly affect the ΔH of the other materials.

3.10. Ion release from the glass

The glass dissolution from composites in PBS was studied by measuring the concentrations of specific ions in PBS (Fig. 12). All composites showed a steady release of ions. 75/25C and 50/50C released a higher amount of ions than 100/0C and 0/100C. 75/25C released more Mg, K, and Si, but 50/50C released more Ca in 24 weeks. 0/100C had the lowest release of all ions.

3.11. Microstructure characterisation

The composites' microstructure was characterised with μ-CT and SEM before and after immersion. The cross-sectional and 3D μ-CT images (Fig. 13 and Fig. 14) and SEM images (Fig. 15) show that the BaG particles are evenly distributed in all composites. Large pores can be seen in the image of 100/0C before immersion (Fig. 13a and 14a). The other composites' structure seems similar, except there is a higher initial amount of BaG in 75/25C than in the other composites.

The composites' volume fractions of BaG particles, polymer matrix, and pores before immersion (Table 9) show that the initial particle fractions of 100/0C, 50/50C, and 0/100C aligned well with the nominal particle fraction, but 75/25C had a slightly higher initial particle fraction than the other composites. The initial porosity of the composites,

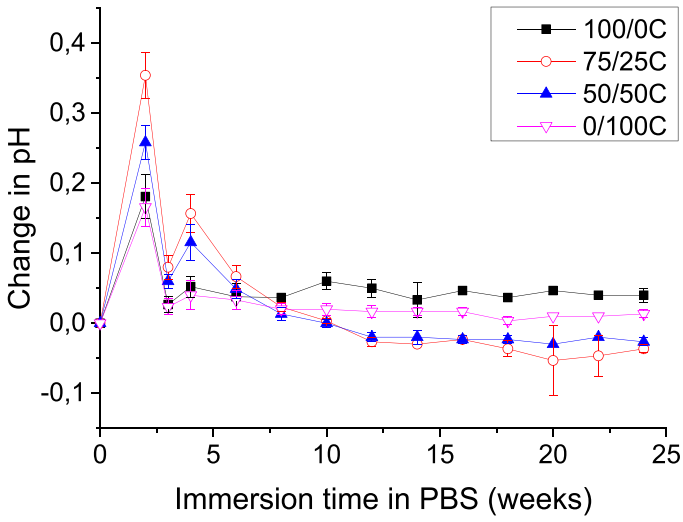

Fig. 5. The pH change of the buffer solution containing PLA/PBSu composites over 24 weeks in PBS. n = 3. The buffer solution was refreshed every two weeks. The results are presented as means with standard deviation.

except 100/0C, was relatively low, ranging from 5 to 6 vol%. 100/0C had a much higher initial porosity (12 vol%) than the other composites.

After 24 weeks in PBS, 100/0C had degraded the most, based on the microstructure analysis. Its BaG content had greatly decreased, and its porosity increased (Fig. 13 e, 14e and 15e). The volume fraction analysis confirmed this; the relative BaG and polymer fractions of 100/0C decreased, and the porosity increased. In addition, the diameter of the 100/0C sample significantly increased during immersion, as seen in Fig. 15e.

After immersion, dark areas on the edges of the BaG particles in the blend composites have appeared, but no other notable visual changes are observed (Fig. 13f-g). However, the volume fractions show that the relative BaG particle volume fraction and porosity have increased, and the polymer fractions decreased during the immersion. The volume fractions of BaG particles, polymer, and pores in 0/100C did not change during the 24-week immersion.

The changes in the glass composition in vitro were assessed with elemental analysis by EDX (Table 10). The initial ratios in the glass align with the glass's nominal composition. After 24 weeks in vitro, the Ca/P ratios at the glass particles' edge were lower than those inside the glass particles in all the studied materials. The difference was more notable in 75/25C, 50/50C, and 0/100C than in 100/0C.

4. Discussion

4.1. Influence of blending on the properties and degradation of polymers

Neat PLA and PBSu, and two PLA/PBSu blends (75/25 and 50/50) were melt processed into rods. A 25/75 blend was also attempted, but the higher temperatures required to melt PLA made the viscosity of PBSu decrease too much when it was the major component in the blend. When processing blends, the temperatures were chosen according to the more thermally stable component because otherwise, it might stay unmolten and block the extruder.

The immiscibility of PLA/PBSu blends is still under debate [39,40]. It most probably depends, among other factors, on the molecular weight difference, crystallinity, processing method used and the proportions of the blend. In general, it seems that PLA/PBSu blends are thermodynamically incompatible, forming two separate phases [41]. PLA has a higher melt viscosity than PBSu, which leads to a higher tendency to form droplets [40]. The ratio of viscosities of the polymer components

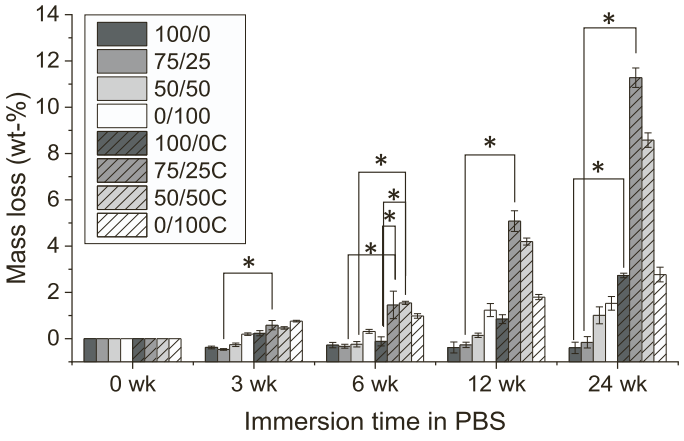

Fig. 7. Sample mass loss over 24 weeks in PBS. * $p < 0.05$. Please note that the y-axis does not start at zero. n = 6. The results are presented as means with standard deviation.

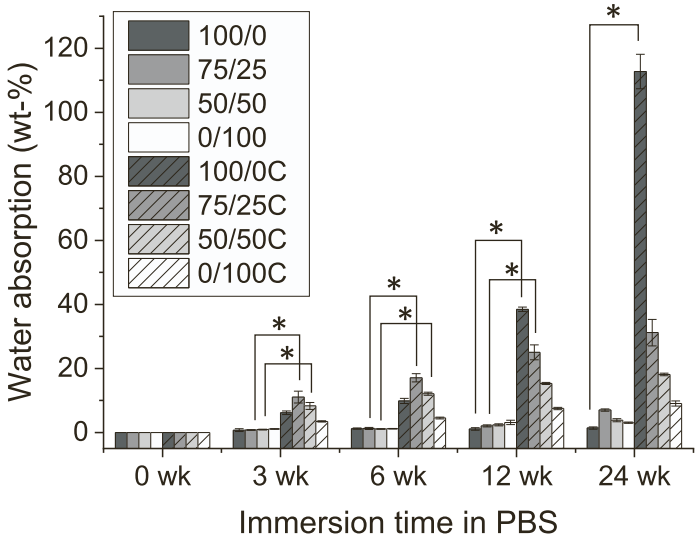

Fig. 6. Water absorption (WA) of the samples over 24 weeks in PBS. * $p < 0.05$. Please note that the y-axis does not start at zero. n = 6. The results are presented as means with standard deviation.

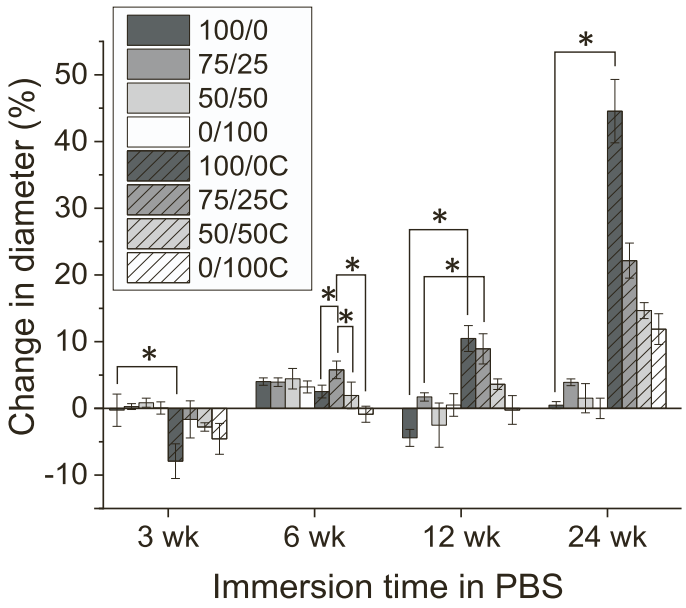

Fig. 8. Changes in the samples' diameter over 24 weeks in PBS. * $p < 0.05$. Please note that the y-axis does not start at zero. n = 6. The results are presented as means with standard deviation.

determines the phase inversion point for the blend. In the current paper, the PLA and PBSu significantly differ in their molecular weights, favouring the sea-island morphology over the formation of a co-continuous phase. Deng and Thomas suggested that when the PBSu content is 10–40 wt%, a co-continuous phase forms between PLA and PBSu. A further increase in PBSu content, namely 50–80 wt%, results in morphology where PLA is dispersed in the PBSu matrix as islets [40].

One of the most used methods to assess polymer miscibility is thermal analysis. Generally, a blend of polymers with poor miscibility would show two distinct glass transitions. In contrast, if the components' miscibility is high, the blend exhibits a single T_g between the glass transitions of the two components [42]. In the current study, the T_g of neat PBSu could not be distinguished, but the observed T_g in the blends lowered from that of neat PLA's. The shift in PLA T_g in the blends indicates partial miscibility. A decrease in PLA T_g in PLA/PBSu blends was also reported earlier [43,44]. The thermograms of the blends showed a single melting peak, but the neat PLA remained amorphous. In addition, the melting enthalpy of the blends was much lower than neat PBSu's, and there was also a shift in the T_m. The shift in T_m could confirm the partial miscibility. However, it can also be assigned to a change in crystal morphology, as reported in [45]. The blends' microstructure in the current report is probably primarily immiscible sea-island morphology, but the lower molecular weight parts of the blends form co-continuous phases. However, the exact microstructure of these blends should be confirmed with further testing.

The interfaces between the blend components may contribute to higher thermal degradation of PLA during blending (Fig. 2). The decrease in molecular weight of 100/0 during processing and gamma irradiation was consistent with our earlier studies [29,31]. The smaller decrease in PBSu molecular weight compared to PLA after gamma irradiation was expected, as PBSu has better radiation resistance than PLA [46].

Kimble and Bhattacharyya [24] also reported a higher molecular weight decrease during PLLA/PBSu blend processing than manufacturing neat PLLA. The decrease was attributed to chain scission during blending. However, it was also stated that they could not distinguish the molecular weights of the individual polymers from the single peak in the GPC chromatogram. Therefore, the lower initial molecular weight of PBSu may distort the molecular weight result of the blends in their results. On the other hand, Zhou et al. [27] did not see differences in the initial molecular weights of PLA and PBSu when in the blends compared to neat PLA and PBSu. They presented the molecular weights of PLA and PBSu separately but did not enclose any details of data analysis.

Blending rigid and brittle PLA with ductile and flexible PBSu decreased the mechanical properties in the blends with increasing PBSu content (Fig. 3), as observed in earlier studies on PLA/PBSu blends [24,27,40,47–53]. The elongation at break was not measured in this study, but it was noted that the non-immersed PBSu-containing samples did not exhibit brittle behaviour during bending testing. However, the dry, sterile, non-immersed 100/0 samples broke in testing.

To further assess the miscibility of the blend, we compared the initial mechanical properties of the blends to the rule of mixture [24]. According to the rule of mixture, the initial bending strengths should be 105.8 and 86.2 MPa, initial modulus 3.2 and 2.5 GPa, and initial shear strengths 43.4 and 39.8 MPa for 75/25 and 50/50, respectively. However, the results in this study are slightly lower, with initial bending strengths of 97.6 and 80.8 MPa, initial modulus 2.8 and 2.1 GPa, and initial shear strengths of 42.1 and 34.2 MPa for 75/25 and 50/50, respectively (Fig. 3). These results support the mainly immiscible microstructure of the blends in the current study.

The hydrolytic degradation of neat PLA, PBSu and PLA/PBSu blends was studied by immersing them in PBS for up to 24 weeks. In general, aliphatic polyesters undergo two-step slow-to-fast hydrolytic degradation. The first step involves random chain scission and decreased molecular weight. When the molecular weight reaches a certain point, the second stage of degradation starts. Then, the low-molecular-weight chain fragments diffuse from the structure, leading to mass loss. [54] In the current study, the neat PLA and PBSu and the PLA/PBSu blends exhibited low water absorption (Fig. 6), negligible mass loss (Fig. 7), and diameter changes (Fig. 8), indicating that the polymers did not reach the second stage of degradation during the study. The slow degradation of PBSu-containing materials was expected, as the hydrolytic degradation of neat PBSu is known to be slow in physiological conditions [55]. In our earlier study, neat PLA also showed negligible degradation in TRIS [29]. In addition, Zhou et al. [27] reported low water absorption and mass loss of neat PLA, PBSu and PLA/PBSu blends after up to 10 months of incubation in SBF.

However, the decreasing mechanical properties may indicate scission of the polymer chains (Figs. 9, 10 and S1). The shear and bending

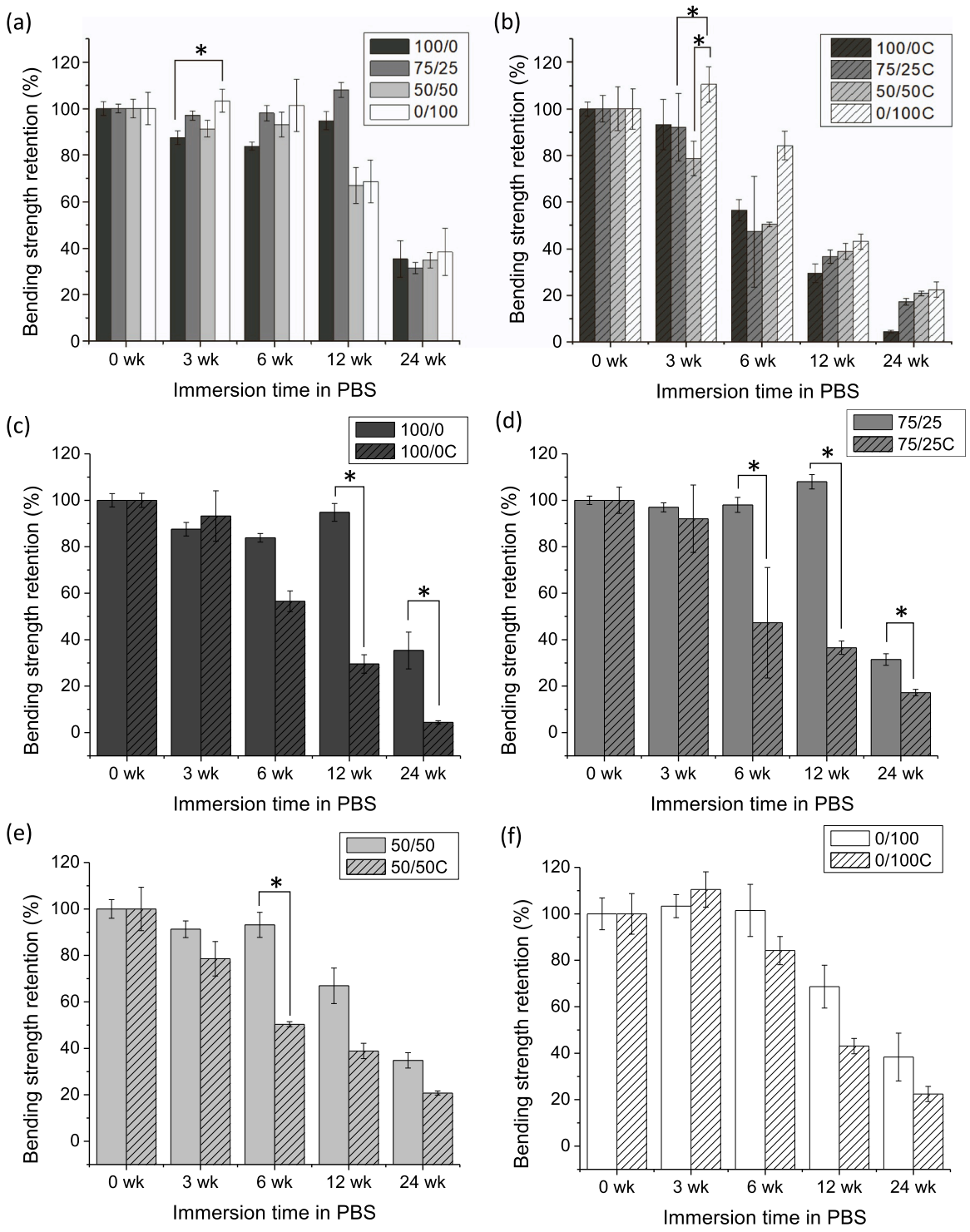

Fig. 9. Bending strength retention of (a) the polymers, (b) the composites, (c)-(f) pairwise comparisons of corresponding polymers and composites over 24 weeks in PBS. * $p < 0.05$. $n = 6$. The results are presented as means with standard deviation.

strength retention of neat PLA was 12 weeks. It was less than in our earlier study, where PLA retained its mechanical properties for 40 weeks in TRIS [29]. However, the samples were gamma-irradiated in the present study, which was not the case in our earlier study. Gamma irradiation degrades the polymers, accelerating their hydrolytic degradation. The shorter bending and shear strength retention of 50/50 compared to the other materials is probably related to the high PBSu content. PBSu becomes more brittle when it degrades. Kimble and Bhattacharyya [24] noticed that after 8 weeks of immersion, the strain of PBSu reduced from 15% to 1%. The increasing brittleness leads to PBSu particles breaking at very low forces and leaving voids in the PLA matrix, weakening the structure.

Kimble and Bhattacharyya [24] reported that injection-moulded PLLA/PBSu blends gradually lost their tensile strength during 24 weeks in vitro in PBS, whereas neat PLA did not. They found that neat PBSu lost its strength much faster than the other materials and concluded that the strength loss of the blends was attributed to the PBSu particles being separated from the PLA matrix and no longer

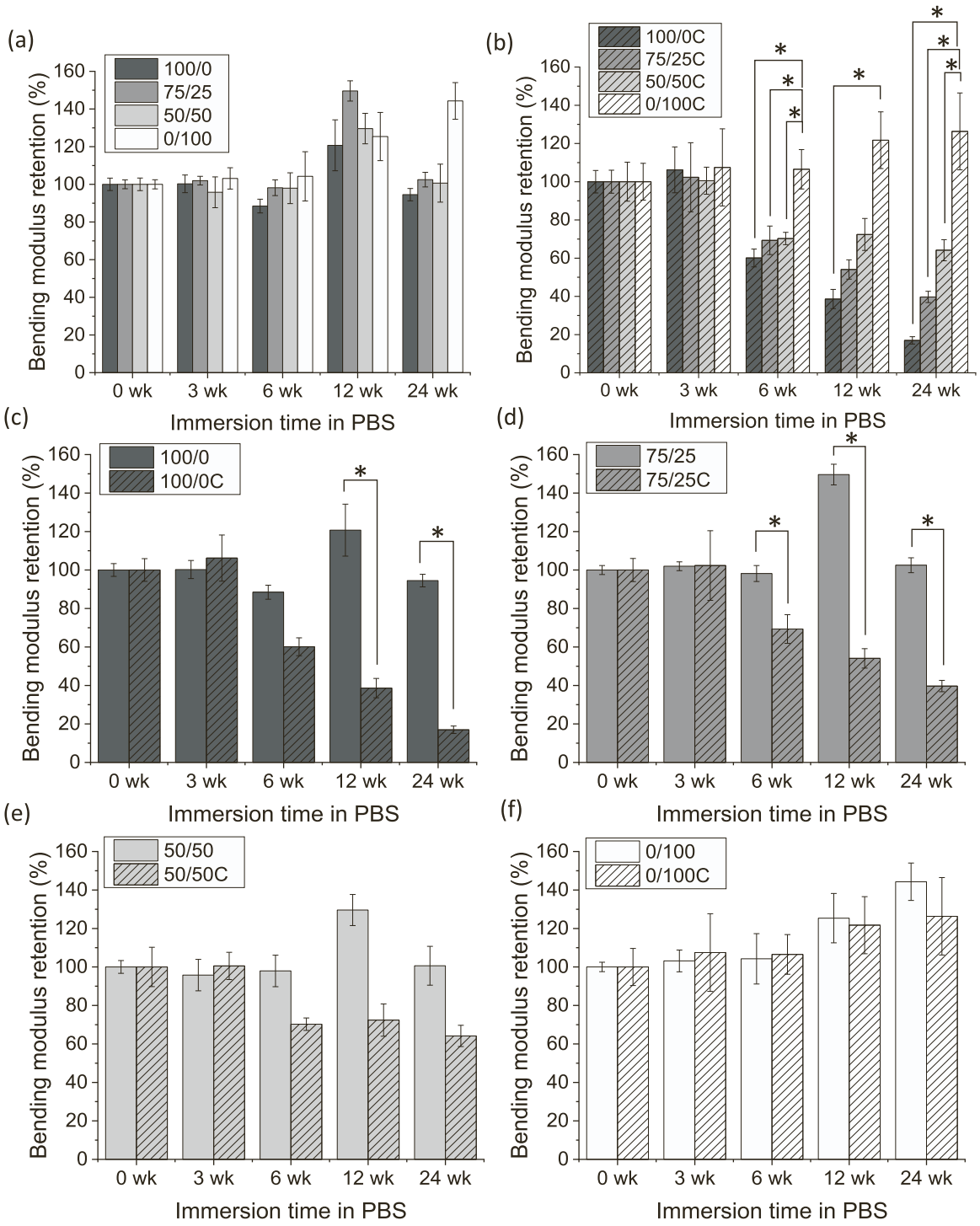

Fig. 10. Bending modulus retention of (a) the polymers, (b) the composites, (c)-(f) pairwise comparisons of corresponding polymers and composites, over 24 weeks in PBS. * $p < 0.05$. $n = 6$. The results are presented as means with standard deviation.

contributing to the strength retention of the material. It has to be taken into account that PLLA is more crystalline than PLDLA used in the present study and, hence, has a slower degradation rate. Zhou et al. [27] reported 60% and 25% tensile strength retention of neat PLA and neat PBSu, respectively, after 6 months in SBF. At the same time point, the blends (20–80% of PBSu) were so degraded that their tensile strength could not be tested. The faster loss of mechanical properties compared to the present study could be attributed to the lower initial molecular weight of the PLA and higher degradation in processing due to two processing steps: melt-mixing and injection moulding.

A higher modulus means the material is stiffer and has a higher resistance to bending. By blending, we could fine-tune the stiffness properties of the blend to be between the parent polymers. It should also be noted that the polymers and blends retained their stiffness for the whole duration of the immersion (24 weeks, Fig. 10). This result is in line with the findings of Kimble and Bhattacharyya [24] for the neat polymers, but in their study, the blends gradually lost their stiffness (Young's modulus) during immersion. The authors conclude that the weakening of the interfacial bonds between the polymer phases in vitro is the reason for the loss of stiffness. They also noticed no relationship

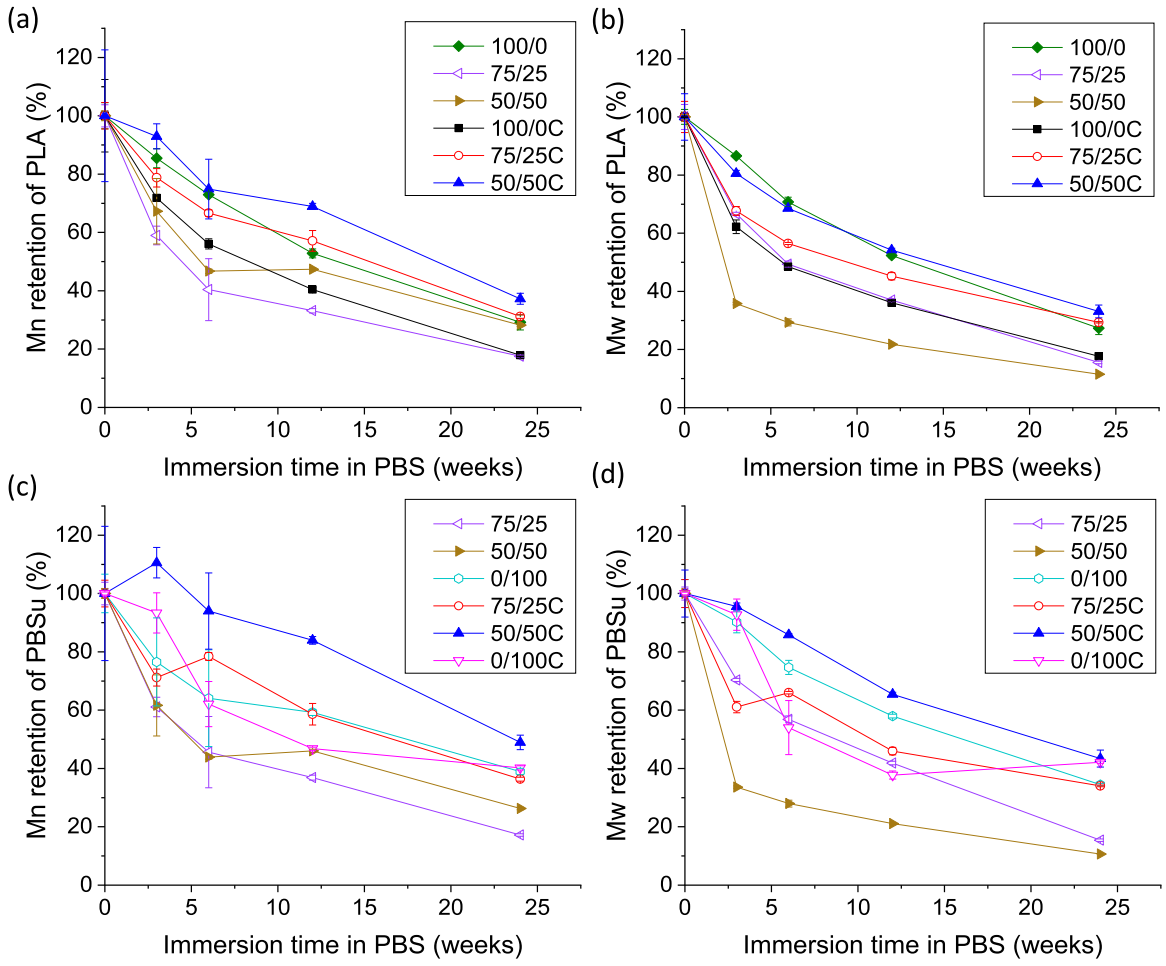

Fig. 11. The number-average (M_n) molecular weight of (a) PLA and (c) PBSu and weight-average (M_w) molecular weight of (b) PLA and (d) PBSu over 24 weeks in PBS. n = 2. The results are presented as means with standard deviation.

between the blending ratios and Young's moduli. Ojansivu et al. [25] also reported no change in Young's modulus and strain at break of neat PLA, PBSu, 95/5, and 75/25 PLA/PBSu blend fibers after four weeks in PBS. However, a direct comparison of the mechanical properties retention cannot be made as there are differences between studies, e.g. in polymer initial molecular weight and processing.

The molecular weight measurements showed that PLA and PBSu degraded faster in the blends (Fig. 11). It was expected, as the thermodynamically incompatible blends have interfacial borders, which enable the water to penetrate the structure better and degrade the material. Kimble and Bhattacharyya [24] measured the M_w of injection moulded neat PLLA and PLLA/PBSu 75/25 blend after immersion in PBS. The neat PLLA lost about 80% and the blend about 95% of their initial molecular weight, respectively, during 24 weeks in PBS. They explain that the chromatograms exhibited only a single peak and that the molecular weights of the single components could not be distinguished.

The thermal analysis showed a decrease in PLA T_g during immersion (Table 7). This decrease is associated with the shortening of the polymer chains [56]. The much higher decrease in T_g in the blends post-immersion results from a faster molecular weight decrease than with neat polymers. After immersion, a cold crystallisation peak emerged in the thermograms of 75/25 and 50/50. Such peaks are known to form when the molecular chains reach a critical length, enabling the crystallisation to occur at temperatures between the T_g and T_m during the heating in the DSC [57]. The 75/25 melting peak exhibited a shoulder at 24 weeks. The higher initial PLA content has probably induced morphological changes in the blend and formation of different crystalline fragments during immersion. In addition, the T_m decreased in 75/25 and 0/100 during immersion, and the ΔH of 0/100 slightly increased (Table 8). The shift in T_m during immersion, as the shift in T_g, is the result of chain shortening. The increase in PBSu melting enthalpy indicates a preferential degradation of the amorphous fragments, leading to a higher crystalline content.

4.2. Properties and degradation of the composites

Manufacturing the composites was successful; the BaG was evenly distributed in the polymer and blend matrices, as seen in the microstructure characterisation (Fig. 14). Additionally, the glass particle fractions in the composites, except 75/25C, were near the nominal value. 75/25C had a higher initial glass particle fraction, as was seen in the inorganic phase content (Table 5) and microstructure analysis results (Table 9). The higher deviation in inorganic phase content of 75/25C leads to higher inaccuracies in the characterisation of properties.

Compounding reactive BaG with PLA increased the thermal degradation of PLA in100/0C compared to 100/0 (Fig. 2). The extent of 100/0C thermal degradation was similar to our previous study [29]. The higher thermal degradation suggests an interaction between PLA and BaG. It should also be noted that the viscosity of PLA decreased when processing 100/0C compared to 100/0, shown as a lower pressure (Table 3). In addition, the porosity of the as-processed 100/0C was higher than the other composites (Table 9). PLA seems more sensitive to BaG than PBSu, but this should be confirmed with additional testing. The negligible effects of BaG addition on the molecular weight decrease

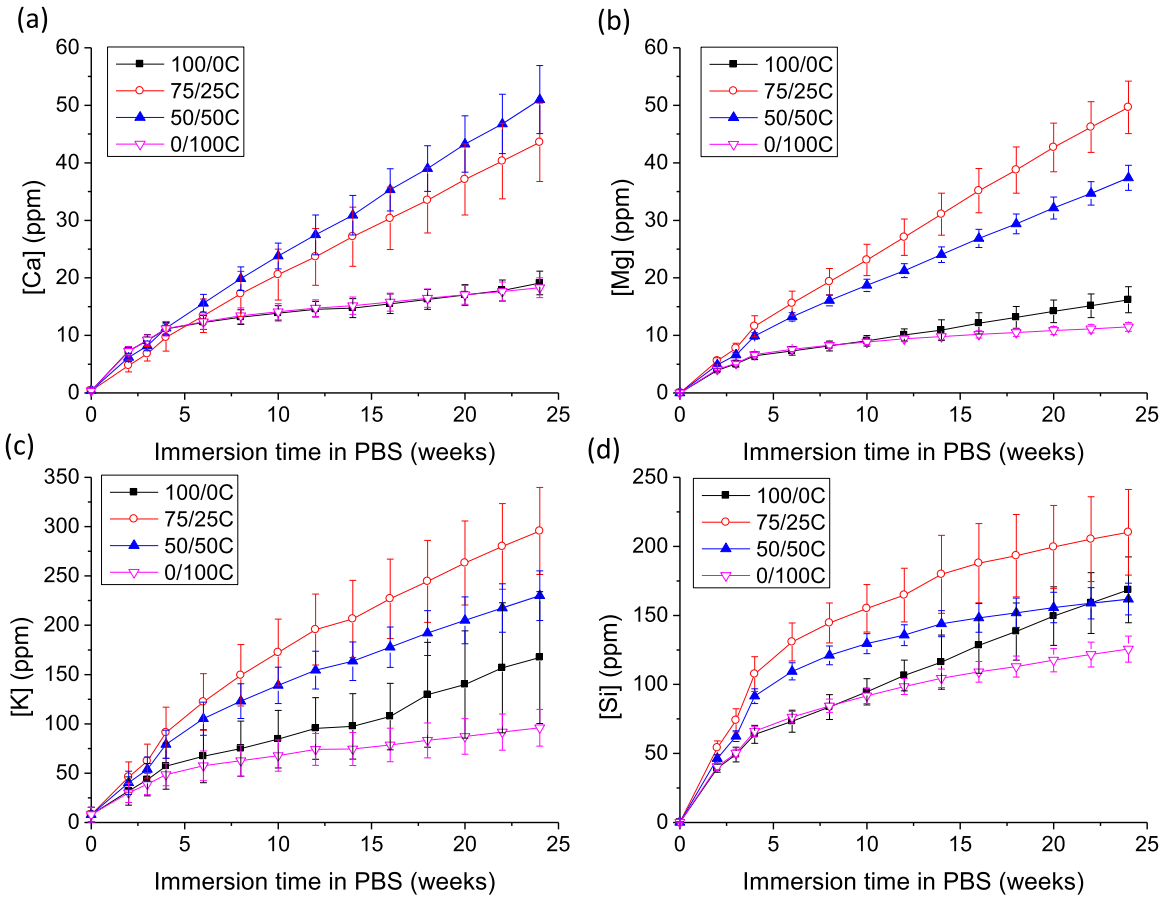

Fig. 12. (a) Calcium (Ca), (b) magnesium (Mg), (c) potassium (K), and (d) silicon (Si) concentration in PBS, as a function of immersion time, for up to 24 weeks. n = 3. The results are presented as means with standard deviation.

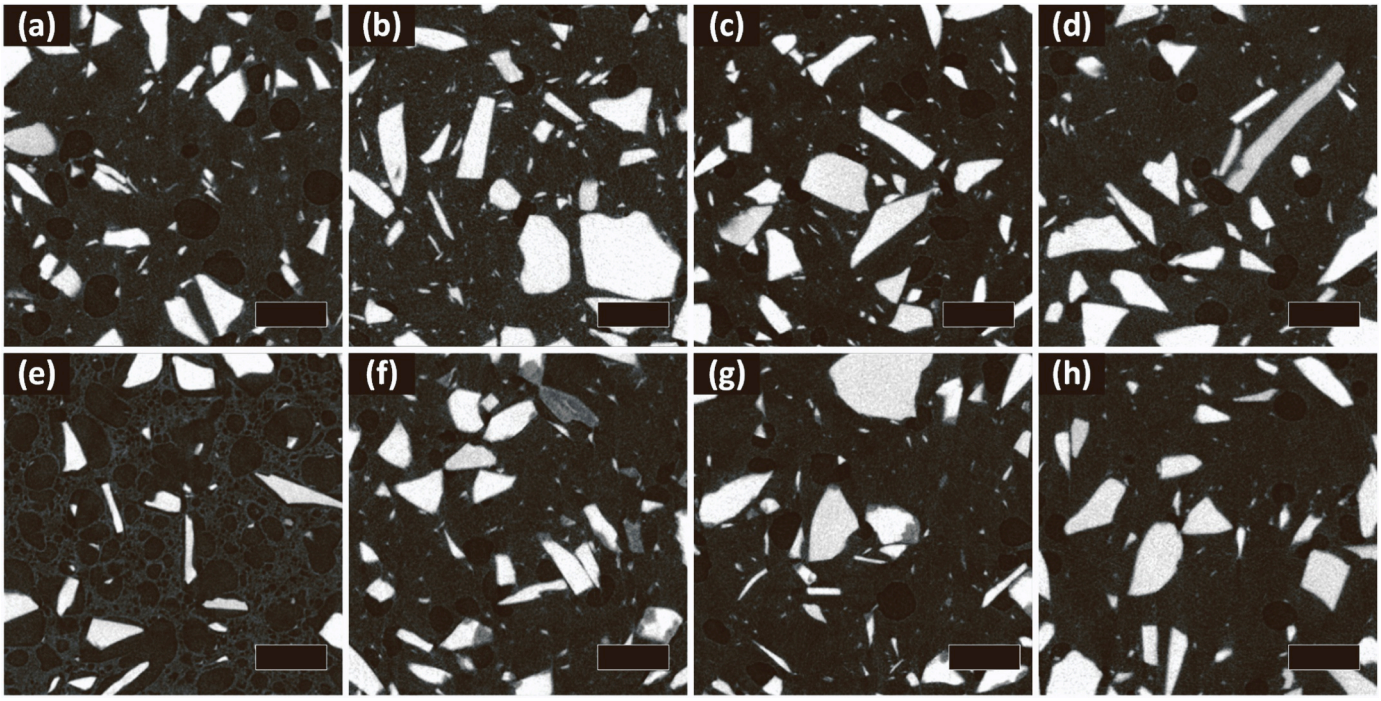

Fig. 13. Cross-sectional μ-CT images of (a) 100/0C, (b) 75/25C, (c) 50/50C and (d) 0/100C before immersion and (e) 100/0C, (f) 75/25C, (g) 50/50C and (h) 0/100C after 24 weeks in PBS. Scale bar 200 μm.

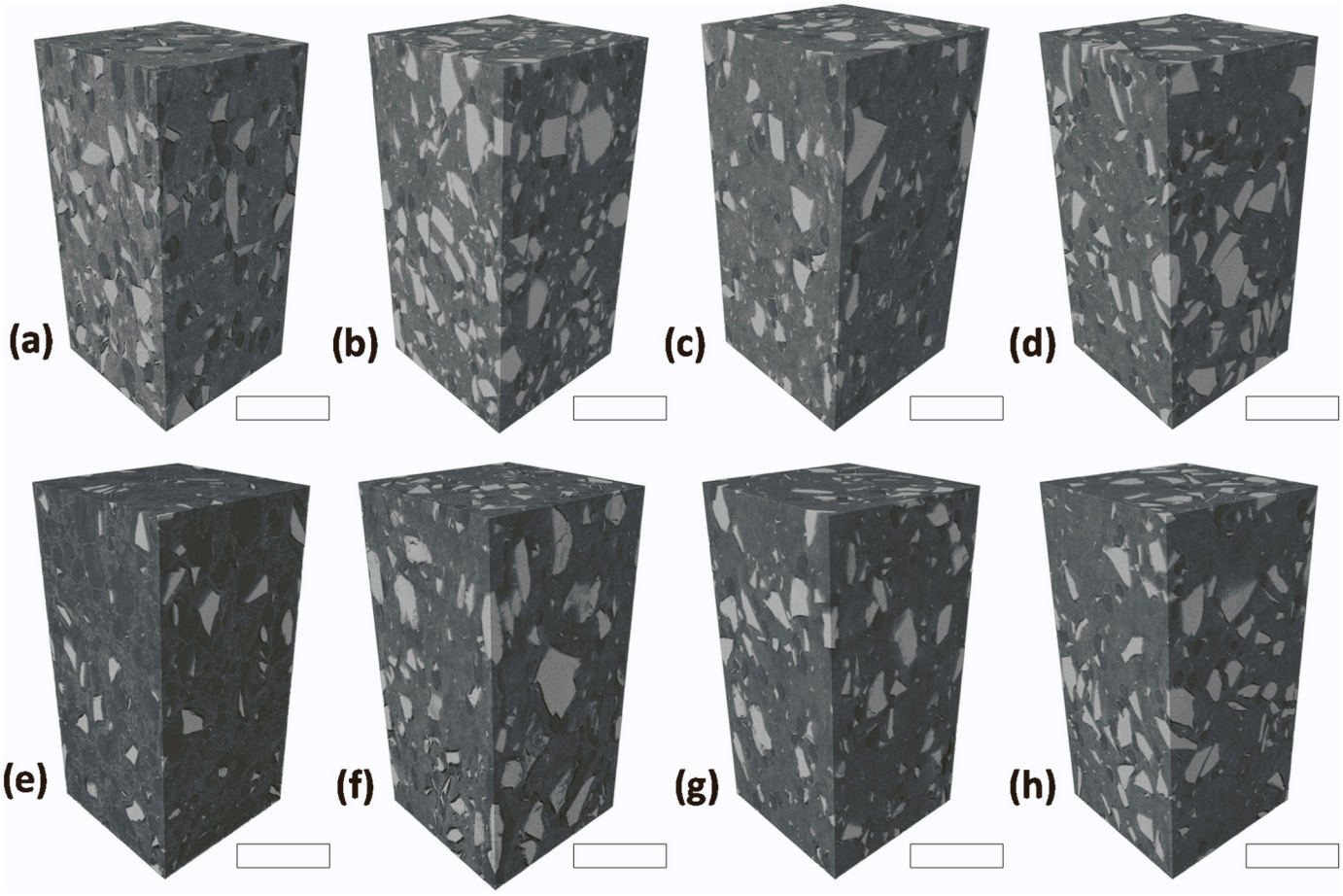

Fig. 14. 3D μ-CT images of (a) 100/0C, (b) 75/25C, (c) 50/50C and (d) 0/100C before immersion and (e) 100/0C, (f) 75/25C, (g) 50/50C and (h) 0/100C after 24 weeks in PBS. Scale bar 500 μm.

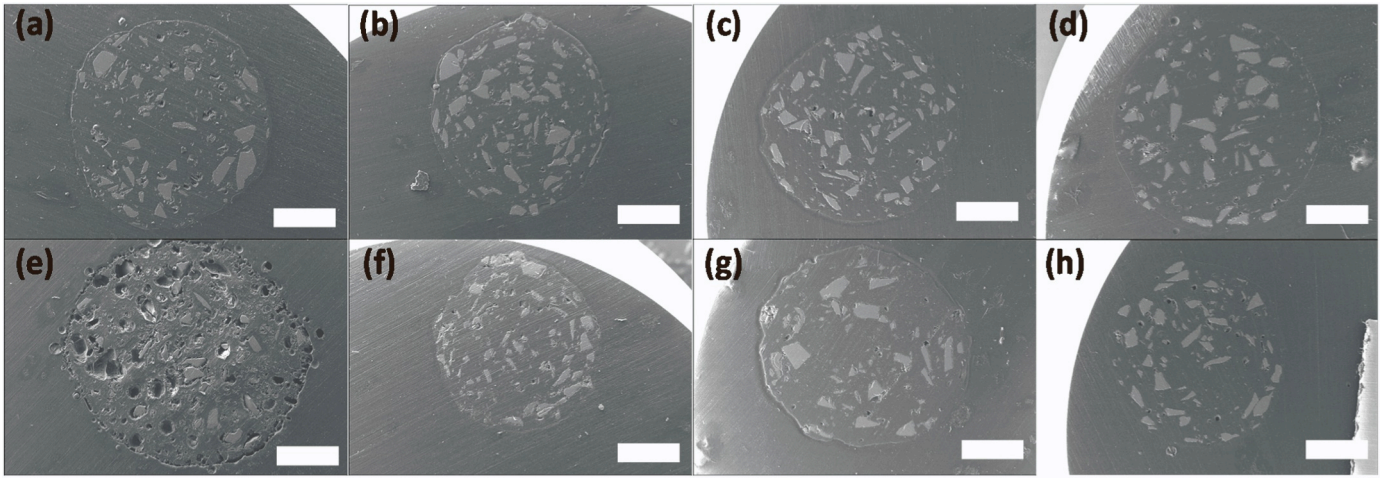

Fig. 15. Representative scanning electron microscopy cross-sectional images of (a) 100/0C, (b) 75/25C, (c) 50/50C, (d) 0/100C before immersion, and (e) 100/0C, (f) 75/25C, (g) 50/50C and (h) 0/100C after 24 weeks in PBS. Scale bar 500 μm.

of PBSu suggest minimal chemical interaction between BaG and PBSu. Accelerated degradation of PLA during processing of PLA/BaG composites has also been reported earlier [58,59]. The hydroxide (OH) or other ions leaching from the glass alter the pH of the melt and affect the degradation of PLA during processing. In addition, some silicate-based BaGs have a high surface energy [60], which leads to water absorbing on the glass surface to form Si-OH (partial glass dissolution in the melt during processing), accelerating PLA's degradation during processing. Nerantzaki et al. reported decreased PBSu molecular weight during two-stage melt polycondensation of PBSu/BaG microparticles [13]. The decrease was attributed to reactions between the hydroxyl and phosphate groups of the BaG and the -COOH or -OH end groups of PBSu. However, the BaG particle size in the current study is much higher (125–250 μm) than the 0.5–3 μm of the study by Nerantzaki et al. The

Table 9
The mean volume fractions of particles, polymers, and porosity of composites before and after immersion in PBS analysed from the μ-CT scans. n = 2. The nominal particle fraction is 17%.

	Volume fractions before immersion						Volume fractions after 24 wk. in PBS					
	Particles		Polymer		Porosity		Particles		Polymer		Porosity	
Sample	Mean	SD	Mean	SD	Mean	SD	Mean	SD	Mean	SD	Mean	SD
100/0C	17	2	72	1	12	0	9	0	45	1	46	0
75/25C	21	2	73	1	6	1	25	3	68	3	7	0
50/50C	16	0	79	1	5	1	22	1	72	2	7	1
0/100C	19	0	77	0	5	0	19	2	76	2	5	0

Table 10
The calculated Ca/P ratios of the composites in atom-% at 24 weeks in vitro compared to the glass only before in vitro. n = 2. The results are presented as means with standard deviation.

	Ca/P ratios before in vitro		Ca/P ratios inside the glass particle, 24 wk. in vitro		Ca/P ratios on BaG/polymer interface, 24 wk. in vitro	
Sample	Mean	SD	Mean	SD	Mean	SD
100/0C	5.9	1.0	5.7	0.8	2.4	0.9
75/25C	5.9	1.0	5.4	0.7	1.2	0.1
50/50C	5.9	1.0	5.7	0.2	1.2	0.1
0/100C	5.9	1.0	5.2	1.3	1.5	0.1

higher particle size leads to decreased reactivity, and maybe the particles were not small enough to induce the reported reactions to such extent that it would affect the PBSu molecular weight.

The thermal analysis showed that BaG did not affect the T_m or T_g of the materials (Table 7 and Table 8). However, BaG induced a cold crystallisation peak in the blends, decreasing the melting enthalpy of all the PBSu-containing materials. These results suggest that the glass particles may disrupt the crystallisation of the polymers and, therefore, influenced the crystals' morphology.

The decrease in mechanical properties when compounding with BaG (Fig. 3) is probably attributed to the weak interfacial bonds between the glass and the polymers. [29,32,61]. The bending modulus was less affected by BaG in all the materials, similar to our previous study [29]. The moduli of the composites could be expected to be higher in composites than polymers because of the addition of a stiffer component. However, in the current work, the porosity and large glass particle size probably impairs the stiffness of the composites. In addition, the bending and shear strength decreases of 100/0C compared to 100/0 were similar to our previous study on PLA/13-93 composites [29]. Compounding with BaG resulted in a similar loss in bending strength, shear strength and PLA's molecular weight in the blend composites as in the corresponding blends, which suggests that BaG did not affect the interactions between the polymer components in the blend composites.

A preliminary assessment of the in vitro reactivity of the composites, namely the formation of a bioactive layer at the material's surface upon immersion, was studied with a 14-day study in SBF. Despite the limitation stated in [55], SBF is generally used as it has similar ion concentrations to blood plasma. The plateau in the release of P could indicate precipitation, but interestingly, this phenomenon was not accompanied by a Ca release change (Fig. 4). However, it should be noted that SBF has a high concentration of Ca. The precipitated CaP probably used up only a negligible amount of Ca compared to the total concentration of Ca in the solution. The higher release of Si with the blend composites compared to the neat polymer composites was probably due to accelerated degradation and a higher number of interfaces in the blend composites. 75/25C had the highest release of Si, attributed to the higher initial BaG content (Table 5 and Table 9).

The hydrolytic degradation of the composites was studied by immersing them in PBS for up to 24 weeks. Incorporating glass into the materials decreased their mechanical properties' retention (Figs. 9, 10 and S1), explained by the increased number of interfaces by the glass particles and the weak bonds between the polymer and the glass. The BaG has also previously been found to decrease the materials' mechanical properties retention [29], [33] due to an increased number of interfaces. In the current study, the increased number of interfaces facilitated water infiltration and resulted in higher WA and mass loss (Figs. 6 and 7) in the composites. Accelerated degradation of PLA/BaG composites compared to neat PLA has also been previously reported and associated with, among other factors, increased hydrophilicity and chemical stress by BaG degradation [13,29,31].

The effect of BaG on the polymer degradation was unexpected; in the blends, it slowed down the molecular weight decrease, but in 100/0C and 0/100C, it caused the molecular weight to decrease faster (Fig. 11). We do not know yet why we see such a trend. The molecular weight decrease was associated with a decrease in PLA T_g, similar to the polymers (Table 7). The melting enthalpies of the polymers during immersion were not altered by BaG in any of the materials, indicating that BaG hindered the degradation of the amorphous regions of the polymers (Table 8).

First, the glass on the surface of the composite rods degraded, which was seen as a pH increase during the first two weeks (Fig. 5). In the early stages of silica glass degradation, it absorbs water to form a silica-rich gel. This phenomenon explains the increase in diameter and higher water absorption of the composites compared to the polymers (Figs. 6 and 8). However, 100/0C absorbed much more water than the other composites and swelled in diameter and length, as seen in the SEM images (Fig. 15). In our earlier study, PLA + 30% 13-93 absorbed 55 wt % water at 20 weeks in Tris [29], about half of the WA of 100/0C in the present study. This high water absorption 100/0C was not anticipated. However, it was associated with a higher degradation rate and initial porosity (Table 9). The pores have facilitated the water penetration into the structure and accelerated the degradation in the bulk of 100/0C. The microstructure analysis showed that after 24 weeks of immersion, most of the glass and polymer in 100/0C had degraded, leaving empty pores in the structure (Fig. 13 and 14, and Table 9). As expected, 100/0C also lost its mechanical properties more quickly than the other materials (Figs. 9, 10 and S1).

It was hypothesised that compounding BaG with the blends would increase the number of interfaces, facilitating water penetration and accelerating the degradation. Further, when the glass and polymer degrade during hydrolysis, they also create voids, which can be filled with water and further advance the degradation. Indeed, the higher degradation rate of the blend composites was seen as a higher increase in pH (Fig. 5), higher mass loss (Fig. 7), and higher ion release (Fig. 12). The higher initial BaG content of 75/25C compared to the other composites (Table 5 and Table 9) also contributed to the higher rise in pH and higher release of ions from the glass.

The microstructure analysis showed that the relative BaG particle volume fractions and porosity of 75/25C and 50/50C increased, and the relative polymer volume fractions decreased during the immersion (Table 9). This suggests polymer degradation and that BaG has mainly transformed into its degradation products but not dissolved to a great extent. These degradation products, probably hydroxy apatite, are seen as dark areas in the BaG particles in the μ-CT images of 75/25C and 50/

50C after 24 weeks of immersion (Fig. 13). The glass reaction with the medium was also confirmed with lower Ca/P ratios at the edge of the glass particles compared to the inside after 24 weeks, indicating more progressed degradation on the particle edges (Table 10).

The BaG had minimal or no effect on the degradation of neat PBSu. As the neat PBSu, the PBSu composite exhibited only minimal degradation. BaG did not affect the bending strength, shear strength, or bending modulus retention of PBSu (Figs. 9, 10 and S1). 0/100C had the lowest release of all ions, and the volume fractions of the particles, polymer, and porosity did not change during the immersion (Fig. 12, Table 9). Probably, this is partly due to the better thermal resistance of PBSu compared to PLA; 0/100C did not degrade thermally as much in the processing as the PLA-containing materials, and therefore, the hydrolytic degradation was not accelerated by the thermal degradation induced in processing (Fig. 2). In addition, 0/100C had the lowest initial porosity of all the composites, which hampers water infiltration (Table 9).

5. Conclusions

To our knowledge, this is the first study evaluating the effect of compounding BaG with PLA/PBSu blends on their hydrolytic degradation. As expected, blending ductile PBSu with rigid PLA decreased the initial mechanical properties as the blends exhibited also PBSu's mechanical behaviour. PBSu and PLA, while being mainly immiscible, exhibit partial miscibility. Blending them creates interfaces that facilitate water penetration in hydrolysis and accelerate the degradation rate, seen as quicker molecular weight decrease and shorter mechanical properties' retention. The neat polymers and blends exhibited negligible mass loss, water absorption and diameter changes, suggesting only minimal degradation within the follow-up period.

Compounding BaG particles with the polymers resulted in decreased initial mechanical properties due to the lack of chemical interactions between the polymers and the glass. It also increased the number of interfaces, which facilitated water infiltration and accelerated especially the degradation of the blend composites. It was seen as a higher increase in pH, higher mass loss and higher ion release to the solution. The early sign of BaG degradation, silica gel formation, was most visible in 100/0C samples. They absorbed a significant amount of water and swelled in both diameter and length, also attributed to the higher initial porosity of 100/0C. Surprisingly, BaG had little effect on the initial properties and degradation rate of neat PBSu.

This study introduces new PLA/PBSu/BaG composites with a wide range of tailorable mechanical properties and degradation rates. The resulting materials exhibited a bending strength of 34–125 MPa, shear strength of 22–47 MPa, bending modulus of 1.1–3.9 GPa, and diverse mechanical properties' retention, water absorption, mass loss, dimensional stability and ion release properties. In addition, the initial assessment of the composites' bioactivity in SBF showed promising signs of precipitation of a bioactive layer. The selection of tailorable properties of these polymer/BaG composites enables their application for tissue engineering of bone to soft tissue.

Funding

This work was supported by TUT Foundation and Business Finland (Human Spare Parts project).

CRediT authorship contribution statement

Inari Lyyra: Conceptualization, Formal analysis, Investigation, Data curation, Writing – original draft, Funding acquisition, Methodology, Validation, Visualisation. **Nina Sandberg:** Investigation. **Vijay Singh Parihar:** Investigation. **Markus Hannula:** Investigation, Formal analysis. **Heini Huhtala:** Formal analysis, Resources, Writing – review & editing. **Jari Hyttinen:** Resources. **Jonathan Massera:** Conceptualization, Methodology, Resources, Writing – review & editing, Supervision, Project administration, Funding acquisition. **Minna Kellomäki:** Conceptualization, Methodology, Validation, Resources, Writing – review & editing, Supervision, Project administration, Funding acquisition. All authors have read and agreed to the published version of the manuscript.

Declaration of Competing Interest

The authors declare that they have no known competing financial interests or personal relationships that could have appeared to influence the work reported in this paper.

Acknowledgements

The authors thank Heikki Liejumäki and Suvi Heinämäki for their valuable help in the laboratory and Terttu Hukka for aid with the GPC analysis. In addition, the authors gratefully acknowledge the Tampere Microscopy Center, especially Turkka Salminen, for the SEM imaging.

Appendix A. Supporting information

Supplementary data associated with this article can be found in the online version at doi:10.1016/j.mtcomm.2023.107242.

References

[1] B.D. Ulery, L.S. Nair, C.T. Laurencin, Biomedical applications of biodegradable polymers, J. Polym. Sci. Part B Polym. Phys. vol. 49 (12) (2011) 832–864, https://doi.org/10.1002/polb.22259.
[2] N. Abay, G. Gurel Pekozer, M. Ramazanoglu, G.T. Kose, Bone formation from porcine dental germ stem cells on surface modified polybutylene succinate scaffolds, Stem Cells Int vol. 2016 (2016), https://doi.org/10.1155/2016/8792191.
[3] X. Zhang, et al., Biodegradable mesoporous calcium–magnesium silicate-polybutylene succinate scaffolds for osseous tissue engineering, Int. J. Nanomed. vol. 10 (2015) 6699–6708, https://doi.org/10.2147/IJN.S92598.
[4] L. Tang, et al., LAPONITE® nanorods regulating degradability, acidic-alkaline microenvironment, apatite mineralization and MC3T3-E1 cells responses to poly (butylene succinate) based bio-nanocomposite scaffolds, RSC Adv. vol. 8 (20) (2018) 10794–10805, https://doi.org/10.1039/c7ra13452e.
[5] Z. Wu, et al., Effects of magnesium silicate on the mechanical properties, biocompatibility, bioactivity, degradability, and osteogenesis of poly(butylene succinate)-based composite scaffolds for bone repair, J. Mater. Chem. B vol. 4 (48) (2016) 7974–7988, https://doi.org/10.1039/c6tb02429g.
[6] X. Tang, et al., Copper-doped nano laponite coating on poly(butylene succinate) scaffold with antibacterial properties and cytocompatibility for biomedical application, J. Nanomater. vol. 2018 (2018), https://doi.org/10.1155/2018/5470814.
[7] S. Patntirapong, W. Janvikul, T. Theerathanagorn, W. Singhatanadgit, Osteoinduction of stem cells by collagen peptide-immobilized hydrolyzed poly (butylene succinate)/β-tricalcium phosphate scaffold for bone tissue engineering, J. Biomater. Appl. vol. 31 (6) (2017) 859–870, https://doi.org/10.1177/0885328216684374.
[8] W. Singhatanadgit, P. Sungkhaphan, T. Theerathanagorn, S. Patntirapong, W. Janvikul, Analysis of sequential dual immobilization of type I collagen and BMP-2 short peptides on hydrolyzed poly(buthylene succinate)/β-tricalcium phosphate composites for bone tissue engineering, J. Biomater. Appl. vol. 34 (3) (2019) 351–364, https://doi.org/10.1177/0885328219852820.
[9] P. Ngamviriyavong, S. Patntirapong, W. Janvikul, S. Arphavasin, P. Meesap, W. Singhatanadgit, Development of poly(butylene succinate)/calcium phosphate composites for bone engineering, Compos. Interfaces vol. 21 (5) (2014) 431–441, https://doi.org/10.1080/15685543.2014.872959.
[10] H. Wang, M. Xu, Z. Wu, W. Zhang, J. Ji, P.K. Chu, Biodegradable poly(butylene succinate) modified by gas plasmas and their in vitro functions as bone implants, ACS Appl. Mater. Interfaces vol. 4 (8) (2012) 4380–4386, https://doi.org/10.1021/am301033t.
[11] D. Zhang, J. Chang, Y. Zeng, Fabrication of fibrous poly(butylene succinate)/wollastonite/apatite composite scaffolds by electrospinning and biomimetic process, J. Mater. Sci. Mater. Med. vol. 19 (1) (2008) 443–449, https://doi.org/10.1007/s10856-006-0043-8.
[12] J. Chen, X. Zhang, B. Li, Y. Yang, Y. Yang, Flexible organic-inorganic hybrid bioceramic for bone tissue regeneration, J. Adv. Dielectr. vol. 10 (4) (2020) 1–7, https://doi.org/10.1142/S2010135×20500137.
[13] M. Nerantzaki, et al., A biomimetic approach for enhancing adhesion and osteogenic differentiation of adipose-derived stem cells on poly(butylene succinate) composites with bioactive ceramics and glasses, Eur. Polym. J. vol. 87 (2017) 159–173, https://doi.org/10.1016/j.eurpolymj.2016.12.014.

[14] S. Patntirapong, W. Singhatanadgit, P. Meesap, T. Theerathanagorn, M. Toso, W. Janvikul, Stem cell adhesion and proliferation on hydrolyzed poly(butylene succinate)/β-tricalcium phosphate composites, J. Biomed. Mater. Res. - Part A vol. 103 (2) (2015) 658–670, https://doi.org/10.1002/jbm.a.35214.
[15] S. Sutthiphong, P. Pavasant, P. Supaphol, Electrospun 1,6-diisocyanatohexane-extended poly(1,4-butylene succinate) fiber mats and their potential for use as bone scaffolds, Polymer vol. 50 (6) (2009) 1548–1558, https://doi.org/10.1016/j.polymer.2009.01.042.
[16] P. Hariraksapitak, O. Suwantong, P. Pavasant, P. Supaphol, Effectual drug-releasing porous scaffolds from 1,6-diisocyanatohexane-extended poly(1,4-butylene succinate) for bone tissue regeneration, Polymer vol. 49 (11) (2008) 2678–2685, https://doi.org/10.1016/j.polymer.2008.04.006.
[17] M. Nerantzaki, et al., Novel poly(butylene succinate) nanocomposites containing strontium hydroxyapatite nanorods with enhanced osteoconductivity for tissue engineering applications, Express Polym. Lett. vol. 9 (9) (2015) 773–789, https://doi.org/10.3144/expresspolymlett.2015.73.
[18] L. Cicero, et al., Polybutylene succinate artificial scaffold for peripheral nerve regeneration, J. Biomed. Mater. Res. - Part B Appl. Biomater. vol. 110 (1) (2022) 125–134, https://doi.org/10.1002/jbm.b.34896.
[19] K. Aliko, M.B. Aldakhlalla, L.J. Leslie, T. Worthington, P.D. Topham, E. Theodosiou, Poly(butylene succinate) fibrous dressings containing natural antimicrobial agents, J. Ind. Text. (2021), https://doi.org/10.1177/1528083720987209.
[20] M.T. Calejo, A. Haapala, H. Skottman, M. Kellomäki, "Porous polybutylene succinate films enabling adhesion of human embryonic stem cell-derived retinal pigment epithelial cells (hESC-RPE), Eur. Polym. J. vol. 118 (January) (2019) 78–87, https://doi.org/10.1016/j.eurpolymj.2019.05.041.
[21] R. Sartoneva, et al., In vitro biocompatibility of polylactide and polybutylene succinate blends for urethral tissue engineering, jbm.b.35268, J. Biomed. Mater. Res. B Appl. Biomater. (2023), https://doi.org/10.1002/jbm.b.35268.
[22] İ.A. Kanneci Altinişik, F.N. Kök, D. Yücel, In vitro evaluation of PLLA/PBS sponges as a promising biodegradable scaffold for neural tissue engineering, Turk. J. Biol. vol. 41 (5) (2017) 734–745, https://doi.org/10.3906/biy-1701-6.
[23] T. Abudula, U. Saeed, A. Memic, K. Gauthaman, M.A. Hussain, H. Al-Turaif, Electrospun cellulose Nano fibril reinforced PLA/PBS composite scaffold for vascular tissue engineering, J. Polym. Res. vol. 26 (5) (2019), https://doi.org/10.1007/s10965-019-1772-y.
[24] L.D. Kimble, D. Bhattacharyya, L.D. Kimble, and D. Bhattacharyya, "In Vitro Degradation Effects on Strength, Stiffness, and Creep of PLLA / PBS: A Potential Stent Material In Vitro Degradation Effects on Strength, Stiffness, and Creep of PLLA = PBS: A Potential Stent Material," vol. 4037, 2015, doi: 10.1080/00914037.2014.945203.
[25] M. Ojansivu, et al., Knitted 3D scaffolds of polybutylene succinate support human mesenchymal stem cell growth and osteogenesis, Stem Cells Int vol. 2018 (2018), https://doi.org/10.1155/2018/5928935.
[26] H. Kun, Z. Wei, L. Xuan, Y. Xiubin, Biocompatibility of a novel poly(butyl succinate) and polylactic acid blend, ASAIO J. vol. 58 (3) (2012) 262–267, https://doi.org/10.1097/MAT.0b013e31824709ee.
[27] J. Zhou, et al., Enhanced mechanical properties and degradability of poly(butylene succinate) and poly(lactic acid) blends, Iran. Polym. J. Engl. Ed (2013) 267–275, https://doi.org/10.1007/s13726-013-0124-8.
[28] Y. Wang, Y. Xiao, J. Duan, J. Yang, Y. Wang, C. Zhang, Accelerated hydrolytic degradation of poly(lactic acid) achieved by adding poly(butylene succinate), Polym. Bull. vol. 73 (4) (2016) 1067–1083, https://doi.org/10.1007/s00289-015-1535-9.
[29] I. Lyyra, K. Leino, T. Hukka, M. Hannula, M. Kellomäki, J. Massera, Impact of glass composition on hydrolytic degradation of polylactide/bioactive glass composites, Materials vol. 14 (3) (2021) 1–20, https://doi.org/10.3390/ma14030667.
[30] T. Niemelä, H. Niiranen, M. Kellomäki, P. Törmälä, Self-reinforced composites of bioabsorbable polymer and bioactive glass with different bioactive glass contents. Part I: initial mechanical properties and bioactivity, Acta Biomater. vol. 1 (2) (2005) 235–242, https://doi.org/10.1016/j.actbio.2004.11.002.
[31] A. Houaoui, I. Lyyra, R. Agniel, E. Pauthe, J. Massera, M. Boissière, Dissolution, bioactivity and osteogenic properties of composites based on polymer and silicate or borosilicate bioactive glass, Mater. Sci. Eng. C. vol. 107 (March 2019) (2020), 110340, https://doi.org/10.1016/j.msec.2019.110340.
[32] H. Niiranen, T. Pyhältö, P. Rokkanen, M. Kellomäki, P. Törmälä, In vitro and in vivo behavior of self-reinforced bioabsorbable polymer and self-reinforced bioabsorbable polymer/bioactive glass composites, J. Biomed. Mater. Res. - Part A vol. 69 (4) (2004) 699–708, https://doi.org/10.1002/jbm.a.30043.
[33] R.M. Felfel, K.M.Z. Hossain, A.J. Parsons, C.D. Rudd, I. Ahmed, Accelerated in vitro degradation properties of polylactic acid/phosphate glass fibre composites, J. Mater. Sci. vol. 50 (11) (2015) 3942–3955, https://doi.org/10.1007/s10853-015-8946-8.
[34] E. Delamarche, A. Mattlet, S. Livi, J.F. Gérard, R. Bayard, V. Massardier, Impact of Ionic Liquids on the (bio)degradability of Poly(butylene succinate)/Poly(lactic acid) blends, Front. Mater. vol. 9 (September) (2022) 1–18, https://doi.org/10.3389/fmats.2022.975438.
[35] J. Brandrup, E.H. Immergut, and E.A. Grulke, Polymer Handbook. Hoboken, NJ, USA: John Wiley & Sons, Ltd, 1999.
[36] A. Schindler, D. Harper, Polylactide. II. Viscosity–molecular weight relationships and unperturbed chain dimensions, J. Polym. Sci. Polym. Chem. Ed. vol. 17 (8) (1979) 2593–2599, https://doi.org/10.1002/pol.1979.170170831.
[37] M. Garin, L. Tighzert, I. Vroman, S. Marinkovic, B. Estrine, "The influence of molar mass on rheological and dilute solution properties of poly(butylene succinate, J. Appl. Polym. Sci. vol. 131 (20) (2014) n/a–n/a, https://doi.org/10.1002/app.40887.
[38] N. Stoyanova, et al., Poly(l-lactide) and poly(butylene succinate) immiscible blends: from electrospinning to biologically active materials, Mater. Sci. Eng. C. vol. 41 (2014) 119–126, https://doi.org/10.1016/j.msec.2014.04.043.
[39] M. Nofar, D. Sacligil, P.J. Carreau, M.R. Kamal, M.C. Heuzey, Poly (lactic acid) blends: processing, properties and applications, Int. J. Biol. Macromol. vol. 125 (2019) 307–360, https://doi.org/10.1016/j.ijbiomac.2018.12.002.
[40] Y. Deng, N.L. Thomas, Blending poly(butylene succinate) with poly(lactic acid): ductility and phase inversion effects, Eur. Polym. J. vol. 71 (2015) 534–546, https://doi.org/10.1016/j.eurpolymj.2015.08.029.
[41] Z. Sun, et al., Influence of polylactide (PLA) stereocomplexation on the microstructure of pla/pbs blends and the cell morphology of their microcellular foams, Polymers vol. 12 (10) (2020) 1–15, https://doi.org/10.3390/polym12102362.
[42] V. Arrighi, J.M. G. Cowie, S. Fuhrmann, and A. Youssef, Miscibility Criterion in Polymer Blends and its Determination. 2016. doi: 10.1002/9783527805204.ch5.
[43] R. Homklin, N. Hongsriphan, Mechanical and thermal properties of PLA/PBS cocontinuous blends adding nucleating agent, Energy Procedia vol. 34 (2013) 871–879, https://doi.org/10.1016/j.egypro.2013.06.824.
[44] R. Wang, S. Wang, Y. Zhang, C. Wan, P. Ma, Toughening modification of PLLA/PBS blends via in situ compatibilization, Polym. Eng. Sci. vol. 49 (1) (. 2009) 26–33, https://doi.org/10.1002/pen.21210.
[45] J.P. Penning, R. St. John Manley, "Miscible blends of two crystalline polymers. 1. Phase behavior and miscibility in blends of poly(vinylidene fluoride) and Poly(1,4-butylene adipate), Macromolecules vol. 29 (1) (1996) 77–83, https://doi.org/10.1021/ma950651t.
[46] M. Negrin, et al., Gamma radiation effects on random copolymers based on poly (butylene succinate) for packaging applications, Radiat. Phys. Chem. vol. 142 (May 2017) (2018) 34–43, https://doi.org/10.1016/j.radphyschem.2017.05.011.
[47] L. Jompang, et al., Poly(lactic acid) and poly(butylene succinate) blend fibers prepared by melt spinning technique, Energy Procedia vol. 34 (2013) 493–499, https://doi.org/10.1016/j.egypro.2013.06.777.
[48] S.B. Park, S.Y. Hwang, C.W. Moon, S.S. Im, E.S. Yoo, Plasticizer effect of novel PBS ionomer in PLA/PBS ionomer blends, Macromol. Res. vol. 18 (5) (2010) 463–471, https://doi.org/10.1007/s13233-010-0512-2.
[49] X. Liu, M. Dever, N. Fair, R.S. Benson, Thermal and mechanical properties of poly (lactic acid) and poly(ethylene/butylene succinate) blends, J. Environ. Polym. Degrad. vol. 5 (4) (1997) 225–235, https://doi.org/10.1007/BF02763666.
[50] T.Y. Qiu, M. Song, L.G. Zhao, Testing, characterization and modelling of mechanical behaviour of poly (lactic-acid) and poly (butylene succinate) blends, Mech. Adv. Mater. Mod. Process. vol. 2 (1) (2016), https://doi.org/10.1186/s40759-016-0014-9.
[51] X. Zhang, Q. Liu, J. Shi, H. Ye, Q. Zhou, "Distinctive tensile properties of the blends of poly(l-lactic acid) (PLLA) and poly(butylene succinate) (PBS), J. Polym. Environ. vol. 26 (4) (2018) 1737–1744, https://doi.org/10.1007/s10924-017-1064-8.
[52] A. Bhatia, R.K. Gupta, H.J. Choi, Compatibility of biodegradable poly (lactic acid) (PLA) and poly (butylene succinate) (PBS) blends for packaging application, Korea-Aust. … vol. 19 (3) (2007) 125–131.
[53] P. Zhao, W. Liu, Q. Wu, J. Ren, Preparation, mechanical, and thermal properties of biodegradable polyesters/poly(Lactic Acid) blends, J. Nanomater. vol. 2010 (2010), https://doi.org/10.1155/2010/287082.
[54] C. Gualandi, et al., Poly(butylene/diethylene glycol succinate) multiblock copolyester as a candidate biomaterial for soft tissue engineering: solid-state properties, degradability, and biocompatibility, J. Bioact. Compat. Polym. vol. 27 (3) (2012) 244–264, https://doi.org/10.1177/0883911512440536.
[55] C. Gualandi, et al., Easily synthesized novel biodegradable copolyesters with adjustable properties for biomedical applications, Soft Matter vol. 8 (20) (2012) 5466, https://doi.org/10.1039/c2sm25308a.
[56] S. Li, Hydrolytic degradation characteristics of aliphatic polyesters derived from lactic and glycolic acids, J. Biomed. Mater. Res. vol. 48 (3) (1999) 342–353, https://doi.org/10.1002/(SICI)1097-4636(1999)48:3<342::AID-JBM20>3.0.CO;2-7.
[57] T. Niemelä, H. Niiranen, M. Kellomäki, Self-reinforced composites of bioabsorbable polymer and bioactive glass with different bioactive glass contents. Part II: in vitro degradation, Acta Biomater. vol. 4 (1) (2008) 156–164, https://doi.org/10.1016/j.actbio.2007.06.007.
[58] J.J. Blaker, A. Bismarck, A.R. Boccaccini, A.M. Young, S.N. Nazhat, Premature degradation of poly(α-hydroxyesters) during thermal processing of Bioglass®-containing composites, Acta Biomater. vol. 6 (3) (2010) 756–762, https://doi.org/10.1016/j.actbio.2009.08.020.
[59] E.H. Backes, L. de, N. Pires, L.C. Costa, F.R. Passador, L.A. Pessan, Analysis of the degradation during melt processing of PLA/biosilicate® composites, J. Compos. Sci. vol. 3 (2) (2019) 52, https://doi.org/10.3390/jcs3020052.
[60] J.J. Blaker, V. Maquet, A.R. Boccaccini, R. Jérôme, A. Bismarck, Wetting of bioactive glass surfaces by poly(α-hydroxyacid) melts: interaction between Bioglass® and biodegradable polymers, E-Polym. no. 023 (2005) 1–13, https://doi.org/10.1515/epoly.2005.5.1.248.
[61] T. Niemelä, Effect of β-tricalcium phosphate addition on the in vitro degradation of self-reinforced poly-L,D-lactide, Polym. Degrad. Stab. vol. 89 (3) (2005) 492–500, https://doi.org/10.1016/j.polymdegradstab.2005.02.003.